

# OPTIMIZATION OF LAMINATED COMPOSITE CYLINDRICAL SHELLS UNDER COMBINED LOADING

*by*

PRAKASH S. TAMHANEY

AE  
1987  
M  
TAM  
OPT



DEPARTMENT OF AERONAUTICAL ENGINEERING  
INDIAN INSTITUTE OF TECHNOLOGY KANPUR

MARCH, 1987

# OPTIMIZATION OF LAMINATED COMPOSITE CYLINDRICAL SHELLS UNDER COMBINED LOADING

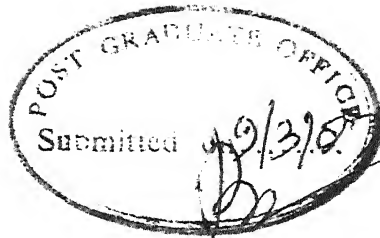
*A Thesis Submitted*  
In Partial Fulfilment of the Requirements  
for the Degree of  
MASTER OF TECHNOLOGY

*by*  
PRAKASH S. TAMHANEY

*to the*  
DEPARTMENT OF AERONAUTICAL ENGINEERING  
INDIAN INSTITUTE OF TECHNOLOGY KANPUR  
MARCH, 1987

30 NOV 1987  
CENTRAL LIBRARY  
\_\_\_\_\_  
Acc. No. A 98878

AE-1987-M-TAM-OPT

CERTIFICATE

This is to certify that the work "OPTIMIZATION OF LAMINATED COMPOSITE CYLINDRICAL SHELLS UNDER COMBINED LOADING" has been carried out under my supervision and has not been submitted elsewhere for a degree.

( V. K. GUPTA )

Assistant Professor

Department of Aeronautical Engineering  
Indian Institute of Technology  
Kanpur

March, 1987

ACKNOWLEDGEMENTS

With great pleasure, I wish to express my profound sense of gratitude to Dr. V.K. Gupta for his invaluable guidance, critical supervision and encouragement throughout the course of this work.

I sincerely thank all of my Hall Four friends, especially Ravi, Sanjay and Bhagirath, who helped me directly or indirectly during the course of this work.

Thanks are also due to Mr. R.N. Srivastava for his quick and neat typing, and Mr. A.K. Ganguly for his fine drafting of the figures.

PRAKASH S. TAMHANEY

CONTENTS

	<u>Page</u>
LIST OF TABLES	vi
LIST OF FIGURES	viii
SYMBOLS AND NOTATION	ix
ABSTRACT	xi
CHAPTER 1 INTRODUCTION AND LITERATURE SURVEY	1
1.1 Brief History and Introduction	1
1.2 Literature Survey	3
1.3 Scope of Present Investigation	8
CHAPTER 2 DEVELOPMENT OF SHELL THEORY	10
2.1 Assumptions of the Theory	10
2.2 Stress Resultant and Stress Couple Relations	12
2.3 Strain-Displacement Relations	13
2.4 Cheng-Ho Equations Governing Buckling of N-layered Laminated Composite Cylindrical Shell	17
2.5 Boundary Conditions	19
2.6 Comparison with Donnell's Theory	20
2.7 Note on Present Theory	22
CHAPTER 3 ANALYSIS AND OPTIMIZATION OF LAMINATED SHELLS	27
3.1 Selection of Displacement Function	27
3.2 Satisfaction of Boundary Conditions	28
3.3 Solution Technique for Long Cylindrical Composite Shells	29
3.4 Optimization	38
3.5 Problem Formulation	38

	Page
3.6 Method of Optimization	39
3.7 Programming Procedure	40
3.7a Steps of Optimization Procedure	41
CHAPTER 4 RESULTS AND DISCUSSION	42
4.1 Critical Buckling Load and Buckling Pattern	43
4.2 Effect of Laminate Configurations on Buckling Load	45
4.3 Effect of Number of Shell Laminae on Buckling Loads	46
4.4 Effect of Ply-angle Orientations on Buckling Loads	47
4.5 Optimum Buckling Loads for Fixed and Variable Lamina Thickness	48
4.6 Effect of Starting Point on Optimal Buckling Loads	50
CHAPTER 5 CONCLUSIONS	73
REFERENCES	76

LIST OF TABLES

Number	Title	Page
4.1	Values of critical buckling loads and buckling patterns for six-layered Boron-Epoxy composite laminated shell under pressure loading	51
4.2	Values of critical buckling loads and buckling pattern for six-layered Boron-Epoxy composite laminated shells under axial compression	52
4.3	Values of critical buckling loads and buckling patterns for six-layered Boron-Epoxy composite laminated shells under torsion	53
4.4	Values of critical buckling loads and buckling pattern for six-layered Boron-Epoxy composite laminated shells under combined axial, pressure and torsional loadings	54
4.5	Critical buckling loads and buckling patterns for a six-layered Boron-Epoxy composite laminated shell subjected to different type of loadings	55
4.6	Values of critical buckling load for three-layered Boron-Epoxy shell ( $K_1 = 1$ , $K_2 = 1$ , $K_3 = 1$ )	56
4.7	Values of critical buckling load for three-layered Boron-Epoxy shell ( $K_1 = 1$ , $K_2 = 1$ , $K_3 = 1$ )	57
4.8	Values of critical buckling load for three-layered Boron-Epoxy shell ( $K_1 = 1$ , $K_2 = 1$ , $K_3 = 1$ )	58
4.9	Variation of critical buckling load with number of shell laminae for cross-ply laminated Boron-Epoxy shells	59
4.10	Variation of buckling load with ply-angle orientations for four-layered carbon epoxy laminated shells	60
4.11	Optimum values of buckling loads for six-layered Boron-Epoxy laminated shells with equal laminae thickness, subject to different loading conditions	61

Number	Title	Page
4.12	Optimum values of buckling loads for six-layered Boron-Epoxy, angle-ply laminated shell subjected to different loading conditions	62
4.13	Effect of starting point on optimal buckling loads and ply-angle orientations for six-layered Boron-Epoxy laminated shell with equal laminae thickness, subjected to axial loading	63
4.14	Effect of starting point on optimal buckling loads, fibre orientations and laminae thickness for six-layered Boron-Epoxy laminated shells under axial loading	64

LIST OF FIGURES

Number	Title	Page
2.1	Cylindrical shell: co-ordinate axes and loads	24
2.2	Force and moment equilibrium for a shell element	25
2.3	Orientation of lamina axes with respect to the reference axes of the shell	26
2.4	Geometry of N-layered composite laminate	26
4.1	Critical buckling load and buckling pattern for six-layered Boron-Epoxy composite shell under pressure loading	65
4.2	Critical buckling load and buckling pattern for six-layered Boron-Epoxy composite shell under axial compression	66
4.3	Critical buckling load and buckling pattern for six-layered Boron-Epoxy composite shell under torsion	67
4.4	Critical buckling load and buckling pattern for six-layered oron-Epoxy composite shell under combined axial compression, pressure and torsion	68
4.5	Effect of various laminate configurations on critical buckling load for 3-layered Boron-Epoxy shell	69
4.6	Effect of various laminate configurations on critical buckling load for 3-layered Boron-Epoxy shell	70
4.7	Effect of number of shell laminae on critical buckling load for cross-ply laminated Boron-Epoxy shell	71
4.8	Effect of ply-angle orientations on critical buckling load for 4-layered carbon epoxy laminated shell	72

### SYMBOLS AND NOTATIONS

$a$	=	radius of shell
$A_{ij}$	=	laminate matrix elements as defined in eqn. (2.11a)
$\bar{A}_{ij}$	=	$A_{ij}/A_{22}$
$B_{ij}$	=	laminate matrix elements as defined in eqn. (2.11b)
$\bar{B}_{ij}$	=	$B_{ij}/aA_{22}$
$C_{ij}$	=	elements of reduced stiffness matrix
$\bar{C}_{ij}$	=	elements of transformed stiffness matrix
$D_{ij}$	=	laminate matrix elements as defined in eqn. (2.11c)
$\bar{D}_{ij}$	=	$D_{ij}/a^2A_{22}$
$e_x, x_\theta, e_{x\theta}$	=	strain components in $x$ and $\theta$ directions
$e_x^o, e_\theta^o, e_{x\theta}^o$	=	mid-plane strain components in $x$ and $\theta$ directions
$E_L$	=	modulus of elasticity in longitudinal direction
$E_T$	=	modulus of elasticity in transverse direction
$G_{LT}$	=	shear modulus of elasticity
$h_k$	=	thickness of $K^{th}$ lamina
$K_1, K_2, K_3$	=	loading factors for different types of loadings
$l$	=	length of shell
$m$	=	number of half wave lengths in axial direction
$M_x, M_\theta, M_{x\theta}, M_{\theta x}$	=	resultant moment components
$n$	=	number of waves in circumferential direction
$N$	=	number of layers of the shell

$N_x, N_\theta, N_{x\theta}, N_{\theta x}$	=	resultant stress components
$p$	=	external pressure load on the shell
$P$	=	axial compression per unit circumferential length
$q_1$	=	$pa/A_{22}$
$q_2$	=	$P/A_{22}$
$q_3$	=	$T/A_{22}$
$T$	=	torsional load per unit circumferential length
$u, v, w$	=	displacements in $x, \theta$ and $z$ directions
$x, \theta, z$	=	reference co-ordinates of midsurface of shell
$\alpha$	=	angle of orientation of fibres with reference $x$ -axis
$\lambda$	=	$m\pi a/l$
$\sigma_x, \sigma_\theta, \sigma_{x\theta}, \sigma_{\theta x}$	=	stress components in $x$ and $\theta$ directions
$X_x, X_\theta, X_{x\theta}$	=	changes in curvature and twist in $x$ and $\theta$ directions
$\nu_{LT}$	=	Poisson's ratio giving strain in transverse direction caused by a strain in longitudinal direction
$\nu_{TL}$	=	Poisson's ratio giving strain in longitudinal direction caused by strain in transverse direction
{ }	=	column matrix
[ ]	=	square or rectangular matrix
,	=	subscript denoting partial differentiation

All other symbols are defined as and when they appear in the thesis.

## ABSTRACT

Cheng and Ho theory for the analysis of laminated composite shells has been used to study the action of combined pressure, axial load and torsional loads. The theory is more involved and gives improved results over Donnell's shell theory.

The solution technique adopted does not allow the satisfaction of boundary conditions; though for long shells the end conditions do not appear to affect the buckling load to a large extent. The study is made for determining the buckling pattern by solution of an eigenvalue problem. Specific values of m-number of half waves along axis of shell and n-number of waves around circumference of shell are found depending on whether loading is single or combined. The effect of laminate configuration, number of laminae and ply-orientations on buckling loads are studied for a shell subjected to all combinations of loading.

Optimization analysis is carried out for six-layered shells with ply-angle and ply-thickness as the design variables. The sequential augmented Lagrangian multiplier method is used for the constrained maximization of buckling load. Study is done for all cases of combined loadings with varying length-to-radius ratios of the shell. The effect of fixed lamina thickness and variable lamina thickness on maximum buckling load is also studied. It is observed that at the optimal point, the laminate configuration turns out to be very close to antisymmetric.

## Chapter 1

### INTRODUCTION AND LITERATURE SURVEY

#### 1.1 Brief History and Introduction:

Shells have been known to be in use for mankind since ages. The abundance of naturally occurring shell structures like bamboo, natural tunnel formations, bird's eggs etc. have indicated the remarkable strength properties and load carrying abilities of such structural elements. As a result of technologically-inclined burgeoning of human interests, a purpose oriented study and experimentation on shell structures has created an area of scientific research which has continuously updated itself with time.

The utility of shell structures like grain storage silos, tunnels, conduits, boilers, architectural domes etc. has highlighted the necessity of developing theories for accurate predictions of behavior of these structures. The parallel improvements in materials for use – and lately the composite materials – have led to highly enhanced applications of shell structures in previously unexplored realms.

The period of 1920s saw the emergence of experimentation in non-conventional structural materials, starting with light-weight, high strength alloys like duralumin, mylar etc. The potentials of such materials, and their drawbacks were realized. This put the designers on a new track of developing materials which would combine better properties of the constituents. For

example, duralumin was found fit by all structural strength demands, but failed where corrosion came into picture. This led to use of wooden chine strip over duralumin shell. It was the first crude attempt using a composite material, which ofcourse failed due to the lack of proper understanding of composite materials at that period in time.

Aerospace structural design requirements of high strength-to-weight ratio and high stiffness-to-weight ratio, made the need for composite materials stronger. This accelerated experimentation on materials in companies, research laboratories and universities all over. World War II brought about an unprecedeted upsurge in practical testing of existing theories. The ramifications in research in the field of shells went on as the quantum of knowledge leaped.

Research on composite materials and composite structures revealed the fact that their design had advantages of high strength-to-weight ratio, durability, ease of repair, design flexibility and high energy absorptivity. Also seamless construction, as is needed for shells, was easily possible. With imperative demands calling up in the development of military aircrafts, jet engines, hypersonic flight and large-distance transportation, strides were taken towards research into chemistry and mechanics of composites.

Research on the problem of buckling of laminated composite shells has been extensively done. With varying degree of approximation, the general theory has been improved upon. Every succeeding improvement is an attempt to reduce simplifying

assumptions and thereby narrow the discrepancies with practical observations. With the availability of high speed computers, it is possible to use a theory employing smaller number of simplifying assumptions. Cheng and Ho [12] theory is one such improvement on Donnell's theory which has been extensively worked upon by many investigators.

### 1.2 Literature Survey:

Budiansky [1] has mathematically formulated the exact tensor equations of equilibrium of isotropic shells. Small perturbation theory to solve the non-linear shell equations has been used. This limits the validity of the theory only for small strains and rotations.

Mah, Almroth and Pittner [2] have done a classical analysis on the stability of cylindrical shells using Donnell's assumptions. Orthotropic as well as ring-stiffened shells have been considered. The loading applied to the shell has been any combination of axial compression, external pressure and torsion. The effects of these combinations on buckling loads of the shells have been studied.

Tennyson [3] has done a photoelastic analysis of isotropic shells subjected to axial compression. This is done with study of high speed photographs (2000 frames/sec) of buckling process taken through a plane reflection type polariscope. Changes in isoclinic pattern with change in buckle wave shape have been recorded as a function of time. Predictions of theory, giving a buckling pattern of wave lengths in

circumferential and axial directions have been verified by this photoelastic analysis.

A small-deflection theory for general instability of orthotropic circular cylindrical shells has been adopted by Becker and Gerard [4]. A solution for the governing differential equations for chosen buckling load conditions has been shown to agree considerably with established data. Ring-stiffened cylinders have also been considered for the purpose of analysis and experimentation.

Dong, Pister and Taylor [5] have postulated a theory for anisotropic plates and shells. They have taken the plate or shell to be composed of an arbitrary number of bonded layers, each possessing different thickness, orientation and elastic properties. Donnell-type equations have been discussed for determining stresses in individual laminae due to bending alone.

Serapico [7] has investigated general instability of reinforced conical and cylindrical shells. The method of solution is based on the principle of minimum potential energy applied to an equivalent orthotropic shell. General results have been reduced to relatively simple formulae and are compared with other investigations and experimental values.

Lowe [8] has presented a method for analysis of stresses in axisymmetrically loaded orthotropic filament wound cylinders. For a case of a circular cylindrical shell with semi-spherical dome, the stress analysis at dome-cylinder junction has been done. Numerical results have been compared to values obtained from hydro-test of a filament wound cylindrical shell.

Dow and Rosen [9] have evaluated the structural efficiency of various materials used in construction of orthotropic shells. A loading-index approach is used in which a measure of structural weight is plotted as a function of an appropriate measure of design load. This is done such that the structure having the least value of ordinate at any value of abscissa is the one giving minimum weight for that design load. A non-dimensional structural efficiency parameter is obtained and plotted for different loading conditions.

Weingarten [10] has studied the effects of pressure on small-deflection buckling of thin-walled cylindrical shells under bending by using modified Donnell's equations. Results indicate the variation of bending stresses with variation of pressure loading.

Direct application of Donnell's equations, adapted by Tsai [6] has been done by Khot [11]. Principle of stationary value of potential energy is used for formulating the buckling equation. Taking restrictions on radius-to-thickness ratio, variation of critical buckling load with configuration of ply-angles is studied for a 3-ply laminated shell. He concludes that configurations of type  $-\theta, 0, \theta$  and  $-\theta, \pi/2, \theta$  at  $\theta \approx 30^\circ$  give maximum critical buckling load and configuration of type  $\theta, -\theta, 0$  and  $\theta, -\theta, \pi/2$  give minimum critical buckling load at  $\theta \approx 90^\circ$ . The value of half wave length in circumferential direction is found to be about 12-16 in all the cases.

Cheng and Ho [12]-[13] used Flügge's equations [20] to develop a more accurate theory for buckling of anisotropic shells.

Assuming a simplified single term solution, they have obtained the solution and tried to satisfy four boundary conditions at the ends of the shell. By performing tests on ply-wood shells, the effectiveness of this theory has been pointed out.

Jones and Morgan [14], using Donnell's approximations have obtained numerical results for cross-ply laminated circular cylindrical shells of boron-epoxy material. A relation between Batdrof shell curvature parameter given as

$$z = \frac{L^2}{rt} \left[ \left\{ 1 - \frac{4\nu^2 E_T^2}{E_L^2} \right\} / \left\{ 1 - \frac{E_T^2}{E_L^2} \right\} \right]^{1/2}$$

and a buckling load parameter  $K_x = - N_x L^2 / \pi^2 D_{11}$  is obtained. An investigation of  $K_x$  with number of layers of shell is done to make the results more practically applicable.

Ugural and Cheng [15] have investigated the buckling of composite cylindrical shells under bending moment using the modified Cheng-Ho [12] theory. Coupling between in-plane stretching and bending is also studied. The numerical results give the variation of buckling load with length-to-radius ratio for the shell, and also the variation of buckling load with ply-angle orientation. Comparison with available data for plywood shells is made. The conclusion that is drawn is that under pure bending effect shells with face layers circumferentially oriented show more resistance to buckling than those face layers which are axially oriented.

Hirano [16] has given a closed-form solution for axisymmetric and axially non-symmetric buckling of angle-ply

laminated circular cylindrical shells with many layers. Loading conditions of uniform axial and compressive loads have been considered.

Whitney and Sun [16] have used Cheng-Ho theory for arriving at an exact solution of buckling equations for an orthotropic laminated composite shell. It is found that though the series solution does not satisfy all the theoretical boundary conditions, the experimental results with simply supported condition are comparable.

Nshanian and Pappas [17] have obtained optimum buckling loads for laminated composite cylinders. The governing equations used are ones with Donnell's approximations. Optimum buckling loads and corresponding optimum ply-angle orientations are obtained for cases of shells with different number of layers and different values of Batdrof parameter  $z$ .

Hirano [19], using Donnell-Tsai approach, has considered the problem of optimization of cylindrical shells under axial compression. The shells are considered to be laminated with  $N$  orthotropic layers, and each layer having the same thickness and equal number of fibres in direction  $\pm\alpha$  with respect to shell axis. By defining buckling stress as a function of buckling-mode parameter the optimum results are obtained for a six-layered shell.

Thus the study of existing literature reveals the following salient features:

- \* Use of simplified Donnell's theory in solution of the buckling equations for shells provides less involved

solution, but at the cost of neglecting the terms representing non-linear interaction between transverse shearing forces and rotations or twisting moments.

- \* A considerable discrepancy exists in the experimental results and numerical results obtained by Donnell's theory.
- \* Optimization is based on the simplified theories, with ply-angle kept as the only design variable.
- \* Using an involved buckling theory, and a detailed solution technique, the comparative study between combined loading effects and other geometric and material properties has not been made so exhaustively.

The following section gives a brief account of the work undertaken and a view of the development of the present thesis.

### 1.3 Scope of Present Investigation:

With the view of approaching practical results for buckling behavior of laminated composite shells, a detailed set of governing equations is used. These equations are solved using a series solution technique. The series terms are assumed such that for all combined loading conditions, simply supported boundary conditions are satisfied as closely as possible. This technique yields a large set of simultaneous equations depending on the terms of the series used.

First part of the present work is the eigenvalue solution of the set of equations, giving the lowest critical buckling load. The values of  $m$  (number of half-waves in axial

direction) and  $n$  (number of waves in circumferential direction) at which the lowest critical buckling load is obtained, give the nature of buckling pattern at those loading conditions.

A direct comparison is made with the existing results and validity of our solution is ensured. During the course of this study it has been possible to obtain new results on combined loading cases. Variation of critical buckling load with respect to angle of orientation of the plies and with respect to different number of layers is also studied.

The second part of work is a study of optimization of six-layered Boron-Epoxy shells under the action of combined loadings. The design variables considered are fibre orientations and individual laminae thickness. Results are obtained for all combinations of loads for the following starting points:

- \* The angles of orientation of each lamina as  $0^\circ$ ,  $30^\circ$ ,  $45^\circ$ ,  $60^\circ$  and  $90^\circ$ .
- \* Cross-ply laminae.
- \* Symmetric angle-ply laminates with the angle configurations of  $[90/0/45]_s$ ,  $[0/0/45]_s$ ,  $[30/45/90]_s$  and  $[15/45/60]_s$ .

The critical buckling load is maximized for preassigned geometry of the shell in terms of its length and radius.

In Chapter 2, the development of shell theory which has been followed here is described. Chapter 3 deals with the solution technique and optimization technique employed. In Chapter 4, results obtained in the present work are presented in graphical form and discussed. Chapter 5 concludes the present study giving the major conclusions drawn.

## Chapter 2

### DEVELOPMENT OF SHELL THEORY

A laminated cylindrical shell consists of a number of layers of thin orthotropic laminae, with the axes of symmetry of each lamina oriented at an arbitrary angle to the shell axis. Consider a laminated cylindrical shell (Figure 2.1), with its geometric axes oriented such that x-axis is defined along the length of the shell, z-axis is defined along the radius and  $\theta$ -axis is defined along the direction perpendicular to x and z axes. Origin of the axes is taken at the centre. The shell with radius 'a' and middle surface as the reference surface, is subjected to combined loading of external pressure  $p$ , axial compression  $P$  per unit of circumference and torque  $T$  per unit of circumferential length.

#### 2.1 Assumptions of the Theory:

Assumptions involved in the development of the theory are summarized as follows:

- 1) The ratio of the thickness of the shell to the radii of curvature of its middle surface is small compared to unity.
- 2) Displacements are very small as compared with the thickness of the shell.
- 3) The straight fibres of an element which are perpendicular to the middle surface before deformation remain so after deformation and do not change their length.

Using these assumptions, the stress-strain relation is obtained from generalized Hooke's law as:

$$\begin{Bmatrix} \sigma_L \\ \sigma_T \\ \sigma_{LT} \end{Bmatrix} = \begin{bmatrix} C_{11} & C_{12} & 0 \\ C_{12} & C_{22} & 0 \\ 0 & 0 & C_{66} \end{bmatrix} \begin{Bmatrix} e_L \\ e_T \\ e_{LT} \end{Bmatrix} \quad (2.1)$$

where  $C_{ij}$  is the reduced stiffness matrix and the elements are

$$C_{11} = E_L / (1 - \nu_{LT} \nu_{TL}) \quad (2.2a)$$

$$C_{12} = E_L \nu_{TL} / (1 - \nu_{LT} \nu_{TL}) \quad (2.2b)$$

$$C_{22} = E_T / (1 - \nu_{LT} \nu_{TL}) \quad (2.2c)$$

$$C_{66} = G_{LT} \quad (2.2d)$$

In general, fibres in a lamina lie at an angle to the laminate reference axes. For the fibres aligned at an angle  $\alpha$  to x-axis of reference plane (Figure 2.4), the transformed stiffness matrix for the  $K^{th}$  lamina is

$$\bar{C}_{ij} = \begin{bmatrix} \bar{C}_{11} & \bar{C}_{12} & \bar{C}_{16} \\ \bar{C}_{12} & \bar{C}_{22} & \bar{C}_{26} \\ \bar{C}_{16} & \bar{C}_{26} & \bar{C}_{66} \end{bmatrix}_K \quad (2.3)$$

where,

$$\bar{C}_{11} = C_{11} \cos^4 \alpha + 2(C_{12} + 2C_{66}) \sin^2 \alpha \cos^2 \alpha + C_{22} \sin^4 \alpha \quad (2.4a)$$

$$\bar{c}_{12} = (c_{11} + c_{22} - 4c_{66})\sin^2\alpha \cos^2\alpha + c_{12}(\sin^4\alpha + \cos^4\alpha) \quad (2.4b)$$

$$\begin{aligned} \bar{c}_{16} &= (c_{11} - c_{12} - 2c_{66})\sin\alpha \cos^3\alpha + (c_{12} - c_{22} \\ &+ 2c_{66})\sin^3\alpha \cos\alpha \end{aligned} \quad (2.4c)$$

$$\bar{c}_{22} = c_{11} \sin^4\alpha + 2(c_{12} + 2c_{66})\sin^2\alpha \cos^2\alpha + c_{22} \cos^4\alpha \quad (2.4d)$$

$$\begin{aligned} \bar{c}_{26} &= (c_{11} - c_{12} - 2c_{66})\sin^3\alpha \cos\alpha + (c_{12} - c_{22} \\ &+ 2c_{66})\sin\alpha \cos^3\alpha \end{aligned} \quad (2.4e)$$

$$\begin{aligned} \bar{c}_{66} &= (c_{11} + c_{22} - 2c_{12} - 2c_{66})\sin^2\alpha \cos^2\alpha + \\ &c_{66}(\sin^4\alpha + \cos^4\alpha) \end{aligned} \quad (2.4f)$$

The applicable Hooke's law now is

$$\left\{ \begin{array}{l} \sigma_L \\ \sigma_T \\ \sigma_{LT} \end{array} \right\} = \begin{bmatrix} \bar{c}_{11} & \bar{c}_{12} & \bar{c}_{16} \\ \bar{c}_{12} & \bar{c}_{22} & \bar{c}_{26} \\ \bar{c}_{16} & \bar{c}_{26} & \bar{c}_{66} \end{bmatrix} \left\{ \begin{array}{l} e_L \\ e_T \\ e_{LT} \end{array} \right\} \quad (2.5)$$

## 2.2 Stress Resultant and Stress Couple Relations:

From the equilibrium of the forces and moments acting on a face of an element of the  $K^{th}$  lamina (Figure 2.2), and defining  $z$  as the radial co-ordinate of the middle surface of a lamina, the stress resultants and stress couples are given by Flügge [20] as:

$$N_x = \int_{-h/2}^{h/2} \sigma_x (1 + \frac{z}{a}) dz \quad (2.6a)$$

$$N_{\theta} = \int_{-h/2}^{h/2} \sigma_{\theta} dz \quad (2.6b)$$

$$N_{x\theta} = \int_{-h/2}^{h/2} \sigma_{x\theta} \left(1 + \frac{z}{a}\right) dz \quad (2.6c)$$

$$N_{\theta x} = \int_{-h/2}^{h/2} \sigma_{\theta x} dz \quad (2.6d)$$

$$M_x = \int_{-h/2}^{h/2} \sigma_x \left(1 + \frac{z}{a}\right) z dz \quad (2.6e)$$

$$M_{\theta} = \int_{-h/2}^{h/2} \sigma_{\theta} z dz \quad (2.6f)$$

$$M_{x\theta} = \int_{-h/2}^{h/2} \sigma_{x\theta} \left(1 + \frac{z}{a}\right) z dz \quad (2.6g)$$

$$M_{\theta x} = \int_{-h/2}^{h/2} \sigma_{\theta x} z dz \quad (2.6h)$$

### 2.3 Strain-Displacement Relations:

The deformation of the cylinder is described by the three components of displacement of any point on the midsurface of the shell. Defining  $u$ ,  $v$  and  $w$  as the displacement of the midsurface in  $x$ ,  $\theta$  and  $z$  directions respectively the strain relations are given by Cheng and Ho [12] as:

$$e_x = u_{,x} - z w_{,xx} \quad (2.7a)$$

$$e_{\theta} = \frac{v_{,\theta}}{a} - \frac{z}{a} \left( \frac{w_{,\theta\theta}}{a+z} \right) + \left( \frac{w}{a+z} \right) \quad (2.7b)$$

$$e_{x\theta} = \left( \frac{u_{,\theta}}{a+z} \right) + \left( 1 + \frac{z}{a} \right) v_{,x} - w_{,x\theta} \left( \frac{z}{a} + \frac{z}{a+z} \right) \quad (2.7c)$$

On expanding  $1/(a + z)$  into power series as

$\frac{1}{a}(1 - \frac{z}{a} + \frac{z^2}{a^2} - \frac{z^3}{a^3} + \dots)$  and neglecting  $z^3/a^3$  and higher order terms, equations (2.7) become:

$$e_x = e_x^0 + z X_z \quad (2.8a)$$

$$e_\theta = e_\theta^0 + z [1 - (z/a)] X_\theta \quad (2.8b)$$

$$e_{x\theta} = [1 + (z^2/2a^2)] e_{x\theta}^0 + z [1 - (z/2a)] X_{x\theta} \quad (2.8c)$$

where the strains at the middle surface of the shell are:

$$e_x^0 = u_x \quad (2.9a)$$

$$e_\theta^0 = (1/a)(v_\theta + w) \quad (2.9b)$$

$$e_{x\theta}^0 = (u_\theta/a) + v_x \quad (2.9c)$$

and the parameters corresponding to the change of curvatures are:

$$X_x = -w_{xx} \quad (2.10a)$$

$$X_\theta = - (1/a^2)(w_{\theta\theta} + w) \quad (2.10b)$$

$$X_{x\theta} = - (2/a)[w_{x\theta} + (u_\theta/2a) - (v_x/2)] \quad (2.10c)$$

For  $K^{th}$  lamina of a shell, the stress-resultants and stress-couples are obtained from equations (2.6), by substituting equations (2.8), (2.9) and (2.10) in equations (2.5) to get stresses in terms of displacements. For a laminated shell with  $N$ -layers, stress resultants and stress couples are obtained by summing for  $N$  laminae. Defining the following stiffness matrices:

$$A_{ij} = \sum_{i=1}^N (\bar{C}_{ij})_k (h_k - h_{k-1}) \quad (2.11a)$$

$$B_{ij} = \frac{1}{2} \sum_{i=1}^N (\bar{C}_{ij})_k (h_k^2 - h_{k-1}^2) \quad (2.11b)$$

$$\text{and } D_{ij} = \frac{1}{3} \sum_{i=1}^N (\bar{C}_{ij}) (h_k^3 - h_{k-1}^3) \quad (2.11c)$$

These are the following expressions:

$$\begin{aligned} N_x &= (A_{11} + \frac{B_{11}}{a}) \{u, x\} + (A_{12} + \frac{B_{12}}{a}) \{\frac{v, \theta}{a} + \frac{w}{a}\} \\ &+ (A_{16} + \frac{B_{16}}{a} + \frac{D_{16}}{a^2}) \{\frac{u, \theta}{a} + v, x\} \\ &+ (B_{11} + \frac{D_{11}}{a}) \{-w, xx\} + B_{12} \{-\frac{w, \theta\theta + w}{a^2}\} \\ &+ (B_{16} + \frac{D_{16}}{2a}) \{-\frac{2w, x\theta}{a} - \frac{u, \theta}{a^2} + \frac{v, x}{a}\} \end{aligned} \quad (2.12a)$$

$$\begin{aligned} N_\theta &= A_{12} \{u, x\} + A_{22} \{\frac{v, \theta}{a} + \frac{w}{a}\} + (A_{26} + \frac{D_{26}}{2a^2}) \{\frac{u, \theta}{a} + v, x\} \\ &+ B_{12} \{-w, xx\} + (B_{22} - \frac{D_{22}}{a}) \{-\frac{w, \theta\theta}{a^2} + \frac{w}{a^2}\} \\ &+ (B_{26} - \frac{D_{26}}{2a}) \{-\frac{2w, x\theta}{a} - \frac{u, \theta}{a^2} + \frac{v, x}{a}\} \end{aligned} \quad (2.12b)$$

$$\begin{aligned} N_{x\theta} &= (A_{16} + \frac{B_{16}}{a}) \{u, x\} + (A_{26} + \frac{B_{26}}{a}) \{\frac{v, \theta}{a} + \frac{w}{a}\} \\ &+ (A_{66} + \frac{B_{66}}{a} + \frac{D_{66}}{a^2}) \{\frac{u, \theta}{a} + v, x\} \end{aligned}$$

$$\begin{aligned}
 & + (B_{16} + \frac{D_{16}}{a}) \{ -w_{xx} \} + B_{26} \{ -\frac{w_{\theta\theta}}{a^2} + \frac{w}{a^2} \} \\
 & + (B_{66} + \frac{D_{66}}{2a}) \{ -\frac{2w_{x\theta}}{a} - \frac{u_{\theta}}{a^2} + \frac{v_x}{a} \} \tag{2.12c}
 \end{aligned}$$

$$\begin{aligned}
 N_{\theta x} & = A_{16} \{ u_x \} + A_{26} \{ \frac{v_{\theta}}{a} + \frac{w}{a} \} + (A_{66} + \frac{D_{66}}{2a}) \{ \frac{u_{\theta}}{a} + v_x \} \\
 & + B_{16} \{ -w_{xx} \} + (B_{26} - \frac{D_{26}}{a}) \{ -\frac{w_{\theta\theta}}{a^2} + \frac{w}{a^2} \} \\
 & + (B_{66} - \frac{D_{66}}{2a}) \{ -\frac{2w_{x\theta}}{a} - \frac{u_{\theta}}{a^2} + \frac{v_x}{a} \} \tag{2.12d}
 \end{aligned}$$

$$\begin{aligned}
 M_x & = (B_{11} + \frac{D_{11}}{a}) \{ u_x \} + (B_{12} + \frac{D_{12}}{a}) \{ \frac{v_{\theta}}{a} + \frac{w}{a} \} \\
 & + (B_{16} + \frac{D_{16}}{a}) \{ \frac{u_{\theta}}{a} + v_x \} + D_{11} \{ -w_{xx} \} \\
 & + D_{12} \{ -\frac{w_{\theta\theta}}{a^2} + \frac{w}{a^2} \} + D_{16} \{ -\frac{2w_{x\theta}}{a} - \frac{u_{\theta}}{a^2} + \frac{v_x}{a} \} \tag{2.12e}
 \end{aligned}$$

$$\begin{aligned}
 M_{\theta} & = B_{12} \{ u_x \} + B_{22} \{ \frac{u_{\theta}}{a} + \frac{w}{a} \} + B_{26} \{ \frac{u_{\theta}}{a} + v_x \} \\
 & + D_{12} \{ -w_{xx} \} + D_{22} \{ -\frac{w_{\theta\theta}}{a^2} + \frac{w}{a^2} \} \\
 & + D_{26} \{ -\frac{2w_{x\theta}}{a} - \frac{u_{\theta}}{a^2} + \frac{v_x}{a} \} \tag{2.12f}
 \end{aligned}$$

$$\begin{aligned}
 M_{x\theta} & = (B_{16} + \frac{D_{16}}{a}) \{ u_x \} + (B_{26} + \frac{D_{26}}{a}) \{ \frac{v_{\theta}}{a} + \frac{w}{a} \} \\
 & + (B_{66} + \frac{D_{66}}{a}) \{ \frac{u_{\theta}}{a} + v_x \} + D_{16} \{ w_{xxx} \}
 \end{aligned}$$

$$+ D_{26} \left\{ \frac{w_{,\theta\theta}}{a^2} + \frac{w}{a^2} \right\} + D_{66} \left\{ -\frac{2w_{,x\theta}}{a} - \frac{u_{,\theta}}{a^2} + \frac{v_{,x}}{a} \right\} \quad (2.12g)$$

$$\begin{aligned} M_{\theta x} = & B_{16} \{u_{,x}\} + B_{26} \left\{ \frac{v_{,\theta}}{a} + \frac{w}{a} \right\} + B_{66} \left\{ \frac{u_{,\theta}}{a} + v_{,x} \right\} \\ & + D_{16} \{-w_{,xxx}\} + D_{26} \left\{ -\frac{w_{,\theta\theta}}{a^2} + \frac{w}{a^2} \right\} \\ & + D_{66} \left\{ -\frac{2w_{,x\theta}}{a} - \frac{u_{,x}}{a^2} + \frac{v_{,x}}{a} \right\} \end{aligned} \quad (2.12h)$$

#### 2.4 Cheng-Ho Equations Governing Buckling of N-layered Laminated Composite Cylindrical Shell:

The differential equations for shell buckling are given by Cheng and Ho [12] as:

$$aN_{x,x} + N_{\theta x,\theta} - p(u_{,\theta\theta} - aw_{,x}) - aPu_{,xx} - 2T u_{,x\theta} = 0 \quad (2.13a)$$

$$\begin{aligned} aN_{\theta,\theta} + a^2 N_{x\theta,x} + M_{\theta,\theta} + aM_{x\theta,x} - pa(v_{,\theta\theta} + w_{,\theta}) - a^2 Pv_{,xx} \\ - 2aT(v_{,x\theta} + w_{,x}) = 0 \end{aligned} \quad (2.13b)$$

$$\begin{aligned} M_{\theta,\theta\theta} + a(M_{x\theta} + M_{\theta x}) + a^2 M_{x,xx} - aN_{\theta} - pa(au_{,x} - v_{,\theta} + w_{,\theta\theta}) \\ - a^2 Pw_{,xx} + 2aT(v_{,x} - w_{,x\theta}) = 0 \end{aligned} \quad (2.13c)$$

Obtaining the derivatives of the terms  $N_{x,x}$ :

$$\begin{aligned} N_{\theta,\theta} ; N_{\theta x,\theta} ; N_{x\theta,x} ; M_{x,xx} ; M_{\theta,\theta} ; M_{x\theta,x} ; M_{\theta,\theta\theta} ; M_{x\theta,x\theta} ; \\ M_{x\theta,\theta x} \text{ and denoting } \bar{A}_{ij} = A_{ij}/A_{22}, \bar{B}_{ij} = B_{ij}/aA_{22}, \bar{D}_{ij} = D_{ij}/a^2 A_{22}, \\ q_1 = pa/A_{22} = k_1 q, \quad q_2 = P/A_{22} = K_2 q, \text{ and } q_3 = T/A_{22} = K_3 q, \end{aligned}$$

the governing equations in terms of the displacements  $u$ ,  $v$  and  $w$  for shell buckling are given as:

$$\begin{aligned}
 & a^2 u_{,xx} (\bar{A}_{11} + \bar{B}_{11}) + 2a u_{,x\theta} \bar{A}_{16} + u_{,\theta\theta} (\bar{A}_{66} - \bar{B}_{66} + \bar{D}_{66}) \\
 & + a^2 v_{,xx} (\bar{A}_{16} + 2\bar{B}_{16} + \bar{D}_{16}) + a v_{,x\theta} (\bar{A}_{12} + \bar{A}_{66} + \bar{B}_{12} + \bar{B}_{66}) \\
 & + v_{,\theta\theta} \bar{A}_{26} - a^3 w_{,xxx} (\bar{B}_{11} + \bar{D}_{11}) - a^2 w_{,xx\theta} (3\bar{B}_{16} + \bar{D}_{16}) \\
 & - aw_{,x\theta\theta} (\bar{B}_{12} + 2\bar{B}_{66} - \bar{D}_{66}) - w_{,\theta\theta\theta} (\bar{B}_{26} - \bar{D}_{26}) + aw_{,x} (\bar{A}_{12}) \\
 & + w_{,\theta} (\bar{A}_{26} - \bar{B}_{26} + \bar{D}_{26}) - q \xi a^2 u_{,xx} K_2 + 2au_{,x\theta} K_3 + \\
 & K_1 (u_{,\theta\theta} - aw_{,x}) \} = 0 \tag{2.14a}
 \end{aligned}$$

$$\begin{aligned}
 & a^2 u_{,xx} (\bar{A}_{16} + 2\bar{B}_{16} + \bar{D}_{16}) + au_{,x\theta} (\bar{A}_{12} + \bar{A}_{66} + \bar{B}_{66} + \bar{B}_{12}) \\
 & + u_{,\theta\theta} (\bar{A}_{26}) + a^2 v_{,xx} (\bar{A}_{66} + 3\bar{B}_{66} + 2\bar{D}_{66}) + 2av_{,x\theta} (\bar{A}_{26} + 2\bar{B}_{26} \\
 & + \bar{D}_{26}) + v_{,\theta\theta} (1 + \bar{B}_{22}) - a^3 w_{,xxx} (\bar{B}_{16} + 2\bar{D}_{16}) \\
 & - a^2 w_{,xx\theta} (\bar{B}_{12} + 2\bar{B}_{66} - \bar{D}_{12} + 3\bar{D}_{66}) - aw_{,x\theta\theta} (3\bar{B}_{26} + 2\bar{D}_{26}) \\
 & - w_{,\theta\theta\theta} \bar{B}_{22} + aw_{,x} (\bar{A}_{26} + \bar{B}_{26}) + w_{,\theta} \\
 & - q \xi a^2 v_{,xx} K_2 + K_3 (2av_{,x\theta} + 2aw_{,x}) + K_1 (v_{,\theta\theta} + w_{,\theta}) \} = 0 \tag{2.14b}
 \end{aligned}$$

$$\begin{aligned}
 & - a^3 u_{,xxx} (\bar{B}_{11} + \bar{D}_{11}) - a^2 u_{,xx\theta} (3\bar{B}_{16} + \bar{D}_{16}) \\
 & - au_{,x\theta\theta} (\bar{B}_{12} + 2\bar{B}_{66} - \bar{D}_{66}) - u_{,\theta\theta\theta} (\bar{B}_{26} - \bar{D}_{26}) + au_{,x} (\bar{A}_{12}) \\
 & + u_{,\theta} (\bar{A}_{26} - \bar{B}_{26} + \bar{D}_{26}) - a^3 v_{,xxx} (\bar{B}_{16} + 2\bar{D}_{16}) - a^2 v_{,xx\theta} (\bar{B}_{12}
 \end{aligned}$$

$$\begin{aligned}
& + 2\bar{B}_{66} + \bar{D}_{12} + 3\bar{D}_{56}) - av,_{x\theta\theta}(3\bar{B}_{26} + 2\bar{D}_{26}) \\
& - v,_{\theta\theta\theta}(\bar{B}_{22}) + av,_{x}(\bar{A}_{26} + \bar{B}_{26}) + v,_{\theta} + a^4 w,_{xxxx}(\bar{D}_{11}) \\
& + 4a^3 w,_{xxx\theta}(\bar{D}_{16}) + 2a^2 w,_{xx\theta\theta}(\bar{D}_{12} + 2\bar{D}_{56}) \\
& + 4aw,_{x\theta\theta\theta}(\bar{D}_{26}) + w,_{\theta\theta\theta\theta}(\bar{D}_{22}) - a^2 w,_{xx}(2\bar{B}_{12}) \\
& - 2aw,_{x\theta}(2\bar{B}_{26} - \bar{D}_{26}) - w,_{\theta\theta}(2\bar{B}_{22} - 2\bar{D}_{22}) \\
& + w(1 - \bar{B}_{22} + \bar{D}_{22}) - q\{K_1(v,_{\theta} - au,_{x} - w,_{\theta\theta}) \\
& + K_2(a^2 w,_{xx}) + K_3(av,_{x} + 2aw,_{x\theta})\} = 0 \tag{2.14c}
\end{aligned}$$

## 2.5 Boundary Conditions:

The governing equations (2.14) are complicated partial differential equations that are to be solved to determine the critical buckling load. The boundary conditions for shell with its edges supported tangentially and radially are given as:

At  $x = \pm 1/2$ ,

$$\begin{aligned}
w = 0 \quad M_x &= B_{11}u,_{x} + D_{11} \frac{u,_{x}}{a} + \frac{B_{12}}{a} v,_{\theta} \\
& + \frac{B_{12}}{a} w + \frac{D_{12}}{a^2} v,_{\theta} + \frac{D_{12}}{a^2} w + \\
& \frac{B_{16}}{a} u,_{\theta} + B_{16} v,_{x} + \frac{D_{16}}{a^2} u,_{\theta} \\
& + D_{16} v,_{x} - D_{11} w,_{xx} - \frac{D_{12}}{a^2} w,_{\theta\theta} - \frac{D_{12}}{a^2} w \\
& - 2 \frac{D_{16}}{a} w,_{x\theta} - \frac{D_{16}}{a^2} u,_{\theta} + \frac{D_{16}}{a} v,_{x} = 0
\end{aligned} \tag{2.15a}$$

Another pair of boundary conditions for the foregoing case is as follows:

If  $v, u \neq 0$  at both ends, then

$$T_x + Pv,_{x} = 0 \quad N_x + Tu,_{\theta}/a = 0 \quad \text{at } x = \pm 1/2 \quad (2.15b)$$

If  $v, u = 0$  at both ends, then

$$v = 0 \quad u = 0 \quad \text{at } x = \pm 1/2 \quad (2.15c)$$

If  $v \neq 0$  and  $u = 0$  at both ends, then

$$T_x + Pv,_{x} = 0 \quad u = 0 \quad \text{at } x = \pm 1/2 \quad (2.15d)$$

If  $v = 0$  and  $u \neq 0$  at both ends, then

$$v = 0 \quad N_x + Tu,_{\theta}/a = 0 \quad \text{at } x = \pm 1/2 \quad (2.15e)$$

where  $T_x = N_{x\theta} + (M_{x\theta}/a)$ .

## 2.6 Comparison with Donnell's Theory:

A major approximation according to Donnell's theory is neglecting all the terms in equations (2.10) except those involving the second derivatives of  $w$ . This leads to a shortcoming that changes in curvature and twist are not fully accounted for. Further assuming the shell to be thin, the terms  $z/a$  in equations (2.6) are neglected compared to unity. Thus the expressions for strains of midsurface are simplified to:

$$e_x = u,_{x} - z w,_{xx} \quad (2.16a)$$

$$e_{\theta} = \frac{v,_{\theta}}{a} + \frac{w}{a} - z \frac{w,_{\theta\theta}}{a^2} \quad (2.16b)$$

$$e_{x\theta} = v,_{x} + \frac{u,_{\theta}}{a} - z \frac{w,_{x\theta}}{a} \quad (2.16c)$$

The stress-resultants and stress-couples are given as:

$$N_x = \int_{-h/2}^{h/2} \sigma_x dz \quad (2.17a)$$

$$N_\theta = \int_{-h/2}^{h/2} \sigma_\theta dz \quad (2.17b)$$

$$N_{x\theta} = N_{\theta x} = \int_{-h/2}^{h/2} \sigma_{x\theta} dz \quad (2.17c)$$

$$M_x = \int_{-h/2}^{h/2} \sigma_x z dz \quad (2.17d)$$

$$M_\theta = \int_{-h/2}^{h/2} \sigma_\theta z dz \quad (2.17e)$$

$$\text{and } M_{x\theta} = M_{\theta x} = \int_{-h/2}^{h/2} \sigma_{x\theta} z dz \quad (2.17f)$$

With these simplifications, the resulting governing equations are obtained on substitution of equations (2.16) and equations (2.17) in equations (2.5). These equations are identical to the ones obtained by Jones [22], and are mentioned here for a direct comparison with the modified form.

$$\begin{aligned}
 & a^2 u_{xx} \bar{A}_{11} + 2au_{x\theta} \bar{A}_{16} + u_{\theta\theta} \bar{A}_{66} + a^2 v_{xx} \bar{A}_{16} \\
 & + av_{x\theta} (\bar{A}_{12} + \bar{A}_{66}) + v_{\theta\theta} \bar{A}_{26} - a^3 w_{xxx} \bar{B}_{11} \\
 & - 3a^2 w_{xx\theta} \bar{B}_{16} - aw_{x\theta\theta} (\bar{B}_{12} + 2\bar{B}_{66}) - w_{\theta\theta\theta} \bar{B}_{26} \\
 & + aw_{x\theta} \bar{A}_{12} + w_{\theta} (\bar{A}_{26}) - qia^2 u_{xx} K_2 + 2au_{x\theta} K_3 \\
 & + K_1 (u_{\theta\theta} - aw_{xx}) \}
 \end{aligned} \quad (2.18a)$$

$$\begin{aligned}
 & a^2 u_{xx} \bar{A}_{16} + a u_{x\theta} (\bar{A}_{12} + \bar{A}_{66}) + u_{\theta\theta} (\bar{A}_{26}) + a^2 v_{xx} \bar{A}_{66} \\
 & + 2av_{x\theta} \bar{A}_{26} + v_{\theta\theta} (1 + \bar{B}_{22}) - a^3 w_{xxx} \bar{B}_{16} - a^2 w_{xx\theta} (\bar{B}_{12} + 2\bar{B}_{66}) \\
 & - aw_{x\theta\theta} (3\bar{B}_{26}) - w_{\theta\theta\theta} \bar{B}_{22} + aw_{x} \bar{A}_{26} + w_{\theta} - q\{a^2 v_{xx} K_2 \\
 & + K_3 (2av_{x\theta} + 2aw_{x}) + K_1 (v_{\theta\theta} + w_{\theta})\} = 0
 \end{aligned} \tag{2.18b}$$

and

$$\begin{aligned}
 & -a^3 u_{xxx} \bar{B}_{11} - 3a^2 u_{xx\theta} \bar{B}_{16} - au_{x\theta\theta} (\bar{B}_{12} + 2\bar{B}_{66}) - u_{\theta\theta\theta} (\bar{B}_{26}) \\
 & + au_{x} \bar{A}_{12} + u_{\theta} (\bar{A}_{26}) - a^3 v_{xxx} (\bar{B}_{16}) - a^2 v_{xx\theta} (\bar{B}_{12} + 2\bar{B}_{66}) \\
 & - 3av_{x\theta} \bar{B}_{26} - v_{\theta\theta\theta} \bar{B}_{22} + av_{x} \bar{A}_{26} + v_{\theta} + a^4 w_{xxxx} \bar{D}_{11} \\
 & + 4a^3 w_{xxx\theta} \bar{D}_{16} + 2a^2 w_{xx\theta\theta} (\bar{D}_{12} + 2\bar{D}_{66}) + 4aw_{x\theta\theta\theta} (\bar{D}_{26}) \\
 & + w_{\theta\theta\theta\theta} \bar{D}_{22} - 2a^2 w_{xx} \bar{B}_{12} - 4aw_{x\theta} \bar{B}_{26} - 2w_{\theta\theta} \bar{B}_{22} + w(1 - \bar{B}_{22}) \\
 & - q\{K_1 (v_{\theta} - au_{x} - w_{\theta\theta}) + K_2 (a^2 w_{xx}) + K_3 (av_{x} + \\
 & 2aw_{x\theta})\} = 0
 \end{aligned} \tag{2.18c}$$

## 2.7 Note on the Present Theory:

Equations (2.14) are very general form of equations for buckling of a laminated cylindrical shell. In these, all the resultant forces and moments are taken into account, and any major assumptions which are likely to lead to deviation of the solution from actual performance, have been eliminated. From Donnell's equations (2.17a,b,c) it is seen that the term  $\bar{A}_{ij}$ ,

$\bar{B}_{ij}$  and  $\bar{D}_{ij}$  appear separately, hence the simplification mentioned below is possible. In the equation

$$\left\{ \begin{array}{c} -N \\ M \end{array} \right\} = \left[ \begin{array}{cc|c} A & & B \\ & B & D \end{array} \right] \left\{ \begin{array}{c} e^0 \\ x \end{array} \right\} \quad (2.19)$$

defining

$$a = [A]^{-1} \quad (2.20a)$$

$$b = [aB] \quad (2.20b)$$

$$\text{and } d = [b^T B - D] \quad (2.20c)$$

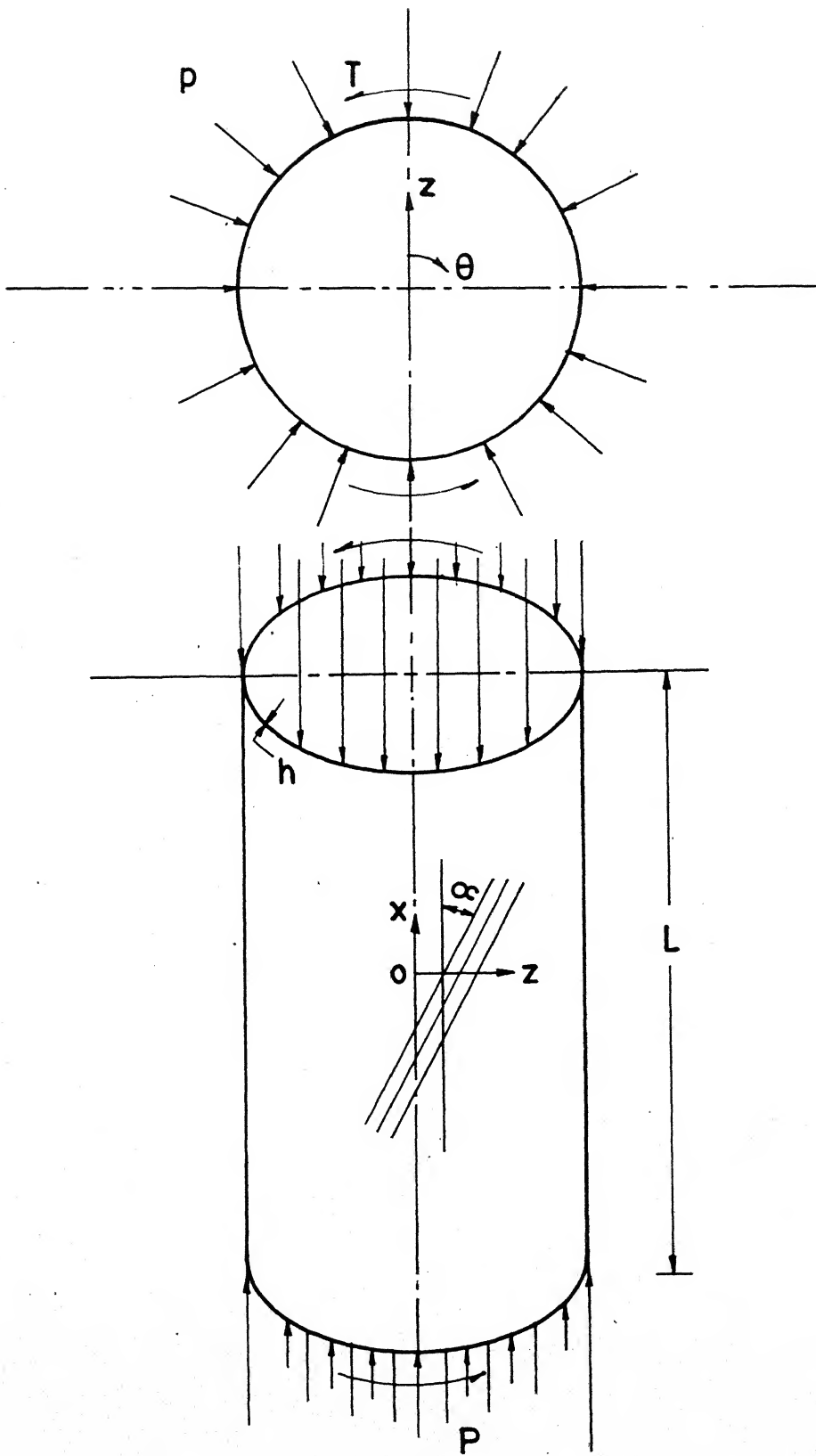
it is possible to obtain two equations of the form

$$\{e^0\} = [a] \{N\} + [b] \{X\} \quad (2.21a)$$

$$\text{and } \{M\} = [b]^T \{N\} + [d] \{X\} \quad (2.21b)$$

Solution of the equilibrium equations (2.13) using equation (2.21) gives the critical buckling load for the shell.

The use of involved Cheng-Ho theory prevents such a solution procedure. Hence it is necessary to assume the displacements of the middle surface as some functions, which is discussed in Chapter 3.



IG. 2.1 CYLINDRICAL SHELL : CO-ORDINATE AXES AND LOADS

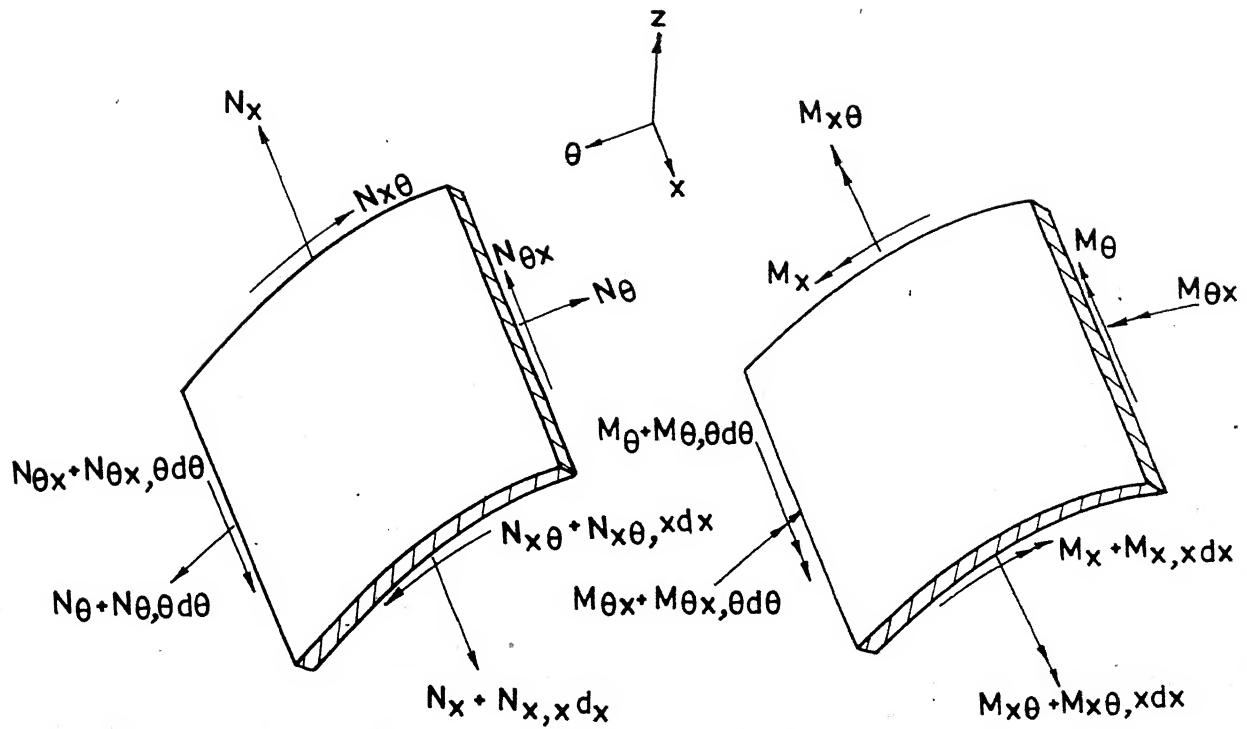


FIG. 2.2 FORCE AND MOMENT EQUILIBRIUM FOR A SHELL ELEMENT

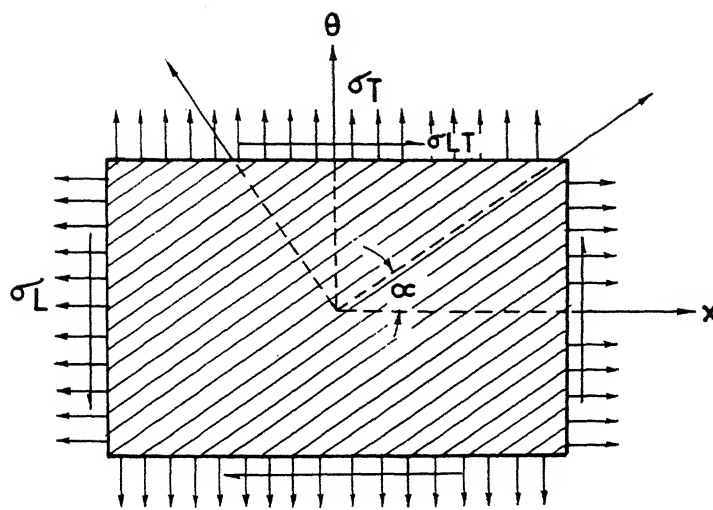


FIG. 2.3 ORIENTATION OF LAMINA AXES WITH RESPECT TO THE REFERENCE AXES OF THE SHELL

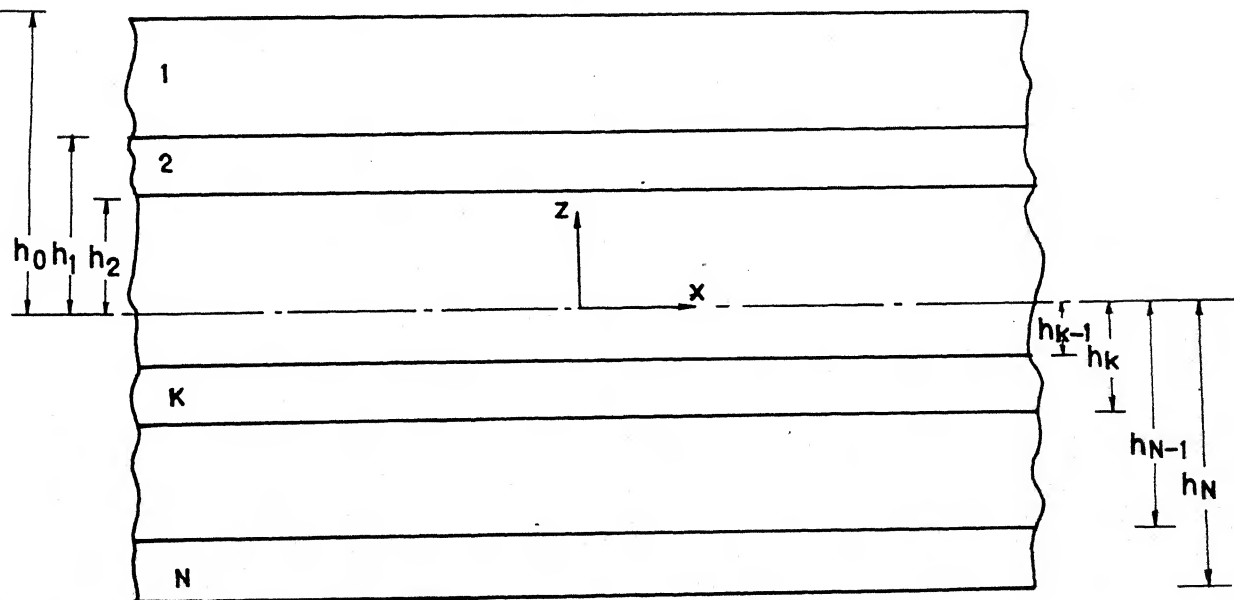


FIG. 2.4 GEOMETRY OF N-LAYERED COMPOSITE LAMINATE.

## Chapter 3

### ANALYSIS AND OPTIMIZATION OF LAMINATED SHELLS

A theoretical analysis for solving the buckling problem of a laminated composite circular cylindrical shell subjected to combined axial, radial and torsional loads is presented in this chapter. The governing equations (2.14) are based on the theory proposed by Cheng and Ho [12] for anisotropic cylindrical shells. By assuming a suitable displacement function for the midsurface displacements, the governing equations reduce to an eigenvalue problem consisting of a set of linear homogeneous algebraic equations. An effective numerical scheme is employed to perform the numerical computations for obtaining the lowest eigenvalue.

As one would like to increase the load carrying capacity of the laminated composite shell for the prescribed geometry and weight, optimization study is undertaken for six-layered shells subjected to axial, radial and torsional loads. The ply-angle and ply-thickness are kept as design variables and buckling load is maximized for the shells of prescribed geometry and weight.

#### 3.1 Selection of Displacement Function:

The assumed displacement function for midsurface displacements should satisfy the governing differential equations (2.14) and boundary conditions (2.15). Since equations (2.14)

are complicated partial differential equations, it is impossible to arrive at an exact solution, using any form of displacement function. Hence a displacement function initially proposed by Flügge [20] and later tested by Cheng and Ho [12], for laminated shell buckling is used in the present work. This displacement function adopted here can be used, for long shells, for all combinations of axial loads, external pressure and torsional loads.

The midsurface displacements in  $x$ ,  $\theta$  and  $z$  directions are assumed as:

$$u = \sum_{n=1}^{\infty} U_n \sin\left(\frac{\lambda x}{a} + n\theta\right) \quad (3.1a)$$

$$v = \sum_{n=1}^{\infty} V_n \sin\left(\frac{\lambda x}{a} + n\theta\right) \quad (3.1b)$$

$$w = \sum_{n=1}^{\infty} W_n \cos\left(\frac{\lambda x}{a} + n\theta\right) \quad (3.1c)$$

$$\text{where } \lambda = \frac{m\pi a}{l} \quad (3.2)$$

This solution describes a buckling mode with  $m$  number of half-waves along axial direction and  $n$  number of waves around circumference of the shell.

### 3.2 Satisfaction of Boundary Conditions:

With the chosen displacement functions for  $u$ ,  $v$  and  $w$ , the boundary conditions to be satisfied for a simply supported shell with origin at centre are given by equations (2.15).

For the condition  $w = M_x = 0$  at  $x = \pm l/2$ , it is not possible to make all the coefficients of stiffness matrices  $A_{ij}$ ,  $B_{ij}$  and  $D_{ij}$  zero for general ply laminates. The displacement conditions given by equation (2.15b) cannot be satisfied for combined loading conditions. However, if the length of the cylinder is very large, then the boundary conditions at the ends do not greatly affect the magnitude of critical stresses. Thus for the length  $l$  assumed to be a part of a much larger cylinder, the solution is not affected by end conditions.

Ugural and Cheng [15] have solved equations (2.14) using a single series solution for the case of pure bending loads for 4-layered ply-wood shells and compared the results with experimental data. Similar procedure is followed here also.

### 3.3 Solution Technique for Long Cylindrical Composite Shells:

The governing equations (2.14) are solved for combined cases of loading, by substituting  $u$ ,  $v$  and  $w$  in the form of equations (3.1). For this it is essential to obtain the derivatives of  $u$ ,  $v$ ,  $w$  upto fourth order. Determining them and using in equations (2.14), one gets:

$$\begin{aligned}
 & \sum_{n=1}^{\infty} [\lambda^2 U_n \sin(\frac{\lambda x}{a} + n\theta) \{ \bar{A}_{11} + \bar{B}_{11} \} + 2n \lambda U_n \sin(\frac{\lambda x}{a} + n\theta) \{ \bar{A}_{16} \} \\
 & + n^2 U_n \sin(\frac{\lambda x}{a} + n\theta) \{ \bar{A}_{66} - \bar{B}_{66} + \bar{D}_{66} \} + \lambda^2 V_n \sin(\frac{\lambda x}{a} + n\theta) \\
 & \{ \bar{A}_{16} + 2\bar{B}_{16} + \bar{D}_{16} \} + \lambda n V_n \sin(\frac{\lambda x}{a} + n\theta) \{ \bar{A}_{12} + \bar{A}_{66} + \bar{B}_{12} + \bar{B}_{66} \} \\
 & + n^2 V_n \sin(\frac{\lambda x}{a} + n\theta) \{ \bar{A}_{26} \} + \lambda^3 W_n \sin(\frac{\lambda x}{a} + n\theta) \{ \bar{B}_{11} + \bar{D}_{11} \}]
 \end{aligned}$$

$$\begin{aligned}
& + \lambda^2 n W_n \sin\left(\frac{\lambda x}{a} + n\theta\right) \{3\bar{B}_{16} + \bar{D}_{16}\} + \lambda n^2 W_n \sin\left(\frac{\lambda x}{a} + n\theta\right) \\
& \{\bar{B}_{12} + 2\bar{B}_{66} - \bar{D}_{66}\} + n^3 W_n \sin\left(\frac{\lambda x}{a} + n\theta\right) \{\bar{B}_{26} - \bar{D}_{26}\} \\
& + \lambda W_n \sin\left(\frac{\lambda x}{a} + n\theta\right) \{\bar{A}_{12}\} + n W_n \sin\left(\frac{\lambda x}{a} + n\theta\right) \{\bar{A}_{26} - \bar{B}_{26} + \bar{D}_{26}\} \\
= & q \sum_{n=1}^{\infty} [\lambda^2 U_n \sin\left(\frac{\lambda x}{a} + n\theta\right) K_2 \\
& + 2\lambda n U_n \sin\left(\frac{\lambda x}{a} + n\theta\right) K_3 + \{n^2 U_n \sin\left(\frac{\lambda x}{a} + n\theta\right) \\
& + \lambda W_n \sin\left(\frac{\lambda x}{a} + n\theta\right)\} K_1] \quad (3.3a)
\end{aligned}$$

$$\begin{aligned}
& \sum_{n=1}^{\infty} [\lambda^2 U_n \sin\left(\frac{\lambda x}{a} + n\theta\right) \{\bar{A}_{16} + 2\bar{B}_{16} + \bar{D}_{16}\} + \lambda n U_n \sin\left(\frac{\lambda x}{a} + n\theta\right) \\
& \{\bar{A}_{12} + \bar{A}_{66} + \bar{B}_{66} + \bar{B}_{12}\} + n^2 U_n \sin\left(\frac{\lambda x}{a} + n\theta\right) \{\bar{A}_{26}\} \\
& + \lambda^2 V_n \sin\left(\frac{\lambda x}{a} + n\theta\right) \{\bar{A}_{66} + 3\bar{B}_{66} + 2\bar{D}_{66}\} \\
& + 2n \lambda V_n \sin\left(\frac{\lambda x}{a} + n\theta\right) \{\bar{A}_{26} + 2\bar{B}_{26} + \bar{D}_{26}\} \\
& + n^2 V_n \sin\left(\frac{\lambda x}{a} + n\theta\right) \{1 + \bar{B}_{22}\} + \lambda^3 W_n \sin\left(\frac{\lambda x}{a} + n\theta\right) \\
& \{\bar{B}_{16} + \bar{D}_{16}\} - \lambda^2 n W_n \sin\left(\frac{\lambda x}{a} + n\theta\right) \{\bar{B}_{12} + 2\bar{B}_{66} - \bar{D}_{12} + 3\bar{D}_{66}\} \\
& + \lambda n^2 W_n \sin\left(\frac{\lambda x}{a} + n\theta\right) \{3\bar{B}_{26} + 2\bar{D}_{26}\} + n^3 W_n \sin\left(\frac{\lambda x}{a} + n\theta\right) \\
& \{\bar{B}_{22}\} + \lambda W_n \sin\left(\frac{\lambda x}{a} + n\theta\right) \{\bar{A}_{26} + \bar{B}_{26}\} - n W_n \sin\left(\frac{\lambda x}{a} + n\theta\right)] \\
= & q \sum_{n=1}^{\infty} [\lambda^2 V_n \sin\left(\frac{\lambda x}{a} + n\theta\right) K_2 \\
& + 2\lambda \{n V_n \sin\left(\frac{\lambda x}{a} + n\theta\right) + W_n \sin\left(\frac{\lambda x}{a} + n\theta\right)\} K_3 \\
& + n \{n V_n \sin\left(\frac{\lambda x}{a} + n\theta\right) + W_n \sin\left(\frac{\lambda x}{a} + n\theta\right)\} K_1] \quad (3.3b)
\end{aligned}$$

and

$$\begin{aligned}
 & \sum_{n=1}^{\infty} \left[ \lambda^3 U_n \cos\left(\frac{\lambda x}{a} + n\theta\right) \{ \bar{B}_{11} + \bar{D}_{11} \} + \lambda^2 n U_n \cos\left(\frac{\lambda x}{a} + n\theta\right) \right. \\
 & \quad \left. \{ 3\bar{B}_{16} + \bar{D}_{16} \} + \lambda n^2 U_n \cos\left(\frac{\lambda x}{a} + n\theta\right) \{ \bar{B}_{12} + 2\bar{B}_{66} - \bar{D}_{66} \} \right. \\
 & \quad \left. + n^3 U_n \cos\left(\frac{\lambda x}{a} + n\theta\right) \{ \bar{B}_{26} - \bar{D}_{26} \} + \lambda U_n \cos\left(\frac{\lambda x}{a} + n\theta\right) \{ \bar{A}_{12} \} \right. \\
 & \quad \left. + n U_n \cos\left(\frac{\lambda x}{a} + n\theta\right) \{ \bar{A}_{26} - \bar{B}_{26} + \bar{D}_{26} \} + \lambda^3 V_n \cos\left(\frac{\lambda x}{a} + n\theta\right) \right. \\
 & \quad \left. \{ \bar{B}_{16} + 2\bar{D}_{16} \} + \lambda^2 n V_n \cos\left(\frac{\lambda x}{a} + n\theta\right) \{ \bar{B}_{12} + 2\bar{B}_{66} + \bar{D}_{12} + 3\bar{D}_{66} \} \right. \\
 & \quad \left. + \lambda n^2 V_n \cos\left(\frac{\lambda x}{a} + n\theta\right) \{ 3\bar{B}_{26} + 2\bar{D}_{26} \} + n^3 V_n \cos\left(\frac{\lambda x}{a} + n\theta\right) \{ \bar{B}_{22} \} \right. \\
 & \quad \left. + \lambda V_n \cos\left(\frac{\lambda x}{a} + n\theta\right) \{ \bar{A}_{26} + \bar{B}_{26} \} + n V_n \cos\left(\frac{\lambda x}{a} + n\theta\right) \right. \\
 & \quad \left. + \lambda^4 W_n \cos\left(\frac{\lambda x}{a} + n\theta\right) \{ \bar{D}_{11} \} + 4\lambda^3 n W_n \cos\left(\frac{\lambda x}{a} + n\theta\right) \{ \bar{D}_{16} \} \right. \\
 & \quad \left. + 2\lambda^2 n^2 W_n \cos\left(\frac{\lambda x}{a} + n\theta\right) \{ \bar{D}_{12} + 2\bar{D}_{66} \} \right. \\
 & \quad \left. + 4\lambda n^3 W_n \cos\left(\frac{\lambda x}{a} + n\theta\right) \{ \bar{D}_{26} \} + n^4 W_n \cos\left(\frac{\lambda x}{a} + n\theta\right) \{ \bar{D}_{22} \} \right. \\
 & \quad \left. + \lambda^2 W_n \cos\left(\frac{\lambda x}{a} + n\theta\right) \{ 2\bar{B}_{12} \} + 2\lambda n W_n \cos\left(\frac{\lambda x}{a} + n\theta\right) \{ 2\bar{B}_{26} - \bar{D}_{26} \} \right. \\
 & \quad \left. + n^2 W_n \cos\left(\frac{\lambda x}{a} + n\theta\right) \{ 2\bar{B}_{22} - 2\bar{D}_{22} \} + W_n \cos\left(\frac{\lambda x}{a} + n\theta\right) \right. \\
 & \quad \left. \{ 1 - \bar{B}_{22} + \bar{D}_{22} \} \right] = q \sum_{n=1}^{\infty} \left\{ \lambda U_n \cos\left(\frac{\lambda x}{a} + n\theta\right) \right. \\
 & \quad \left. + n V_n \cos\left(\frac{\lambda x}{a} + n\theta\right) + n^2 W_n \cos\left(\frac{\lambda x}{a} + n\theta\right) \right\} K_1 \\
 & \quad + \lambda^2 \cos\left(\frac{\lambda x}{a} + n\theta\right) K_2 + 2\lambda \left\{ V_n \cos\left(\frac{\lambda x}{a} + n\theta\right) \right. \\
 & \quad \left. + n W_n \cos\left(\frac{\lambda x}{a} + n\theta\right) \right\} K_3 \quad (3.3c)
 \end{aligned}$$

Equations (3.3) are rewritten in the following form by collecting the coefficients of  $U_n$ ,  $V_n$  and  $W_n$ :

$$\sum_{n=1}^{\infty} [U_n a_{11} + V_n a_{12} + W_n a_{13} - q \{ U_n b_{11} + V_n b_{12} + W_n b_{13} \}] \sin\left(\frac{\lambda x}{a} + n\theta\right) = 0 \quad (3.4a)$$

$$\sum_{n=1}^{\infty} [U_n a_{21} + V_n a_{22} + W_n a_{23} - q \{ U_n b_{21} + V_n b_{22} + W_n b_{23} \}] \sin\left(\frac{\lambda x}{a} + n\theta\right) = 0 \quad (3.4b)$$

and,

$$\sum_{n=1}^{\infty} [U_n a_{31} + V_n a_{32} + W_n a_{33} - q \{ U_n b_{31} + V_n b_{32} + W_n b_{33} \}] \cos\left(\frac{\lambda x}{a} + n\theta\right) = 0 \quad (3.4c)$$

where,

$$a_{11} = (\bar{A}_{11} + \bar{B}_{11}) \lambda^2 + 2\bar{A}_{16} \lambda n + (\bar{A}_{66} + \bar{B}_{66} - \bar{D}_{66}) n^2 \quad (3.5a)$$

$$a_{12} = (\bar{A}_{16} + 2\bar{B}_{16} + \bar{D}_{16}) \lambda^2 + (\bar{A}_{12} + \bar{A}_{66} + \bar{B}_{12} + \bar{B}_{66}) \lambda n + \bar{A}_{26} n^2 \quad (3.5b)$$

$$a_{13} = (\bar{B}_{11} + \bar{D}_{11}) \lambda^3 + (3\bar{B}_{16} + \bar{D}_{16}) \lambda^2 n + [(\bar{B}_{12} + 2\bar{B}_{66} - \bar{D}_{66}) n^2 + \bar{A}_{12}] \lambda + (\bar{B}_{26} - \bar{D}_{26}) n^3 + (\bar{A}_{26} - \bar{B}_{26} + \bar{D}_{26}) n \quad (3.5c)$$

$$a_{21} = (\bar{A}_{16} + 2\bar{B}_{16} + \bar{D}_{16}) \lambda^2 + (\bar{A}_{12} + \bar{A}_{66} + \bar{B}_{12} + \bar{B}_{66}) n + \bar{A}_{26} n^2 \quad (3.5d)$$

$$\begin{aligned}
 a_{22} = & (\bar{A}_{66} + 3\bar{B}_{66} + 3\bar{D}_{66})\lambda^2 + (\bar{A}_{26} + 2\bar{B}_{26} + \bar{D}_{26})2n\lambda \\
 & + (1 + \bar{B}_{22})n^2
 \end{aligned} \tag{3.5e}$$

$$\begin{aligned}
 a_{23} = & (\bar{B}_{16} + 2\bar{D}_{16})\lambda^3 + (\bar{B}_{12} + 2\bar{B}_{66} + \bar{D}_{12} + 3\bar{D}_{66})\lambda^2n \\
 & + [(3\bar{B}_{26} + 2\bar{D}_{26})n^2 + \bar{A}_{26} + \bar{B}_{26}]\lambda + \bar{B}_{22}n^3 + n
 \end{aligned} \tag{3.5f}$$

$$\begin{aligned}
 a_{31} = & (\bar{B}_{11} + \bar{D}_{11})\lambda^3 + (3\bar{B}_{16} + \bar{D}_{16})\lambda^2n + \\
 & [(\bar{B}_{12} + 2\bar{B}_{66} - \bar{D}_{66})n^2 + \bar{A}_{12}]\lambda + (\bar{B}_{26} - \bar{D}_{26})n^3 \\
 & + (\bar{A}_{26} - \bar{B}_{26} + \bar{D}_{26})n
 \end{aligned} \tag{3.5g}$$

$$\begin{aligned}
 a_{32} = & (\bar{B}_{16} + 2\bar{D}_{16})\lambda^3 + (\bar{B}_{12} + 2\bar{B}_{66} + \bar{D}_{12} + 3\bar{D}_{66})\lambda^2n \\
 & + [(3\bar{B}_{26} + 2\bar{D}_{26})n^2 + \bar{A}_{26} + \bar{B}_{26}]\lambda + \bar{B}_{22}n^3 + n
 \end{aligned} \tag{3.5h}$$

$$\begin{aligned}
 a_{33} = & \bar{D}_{11}\lambda^4 + \bar{D}_{16}4\lambda^3n + [(\bar{D}_{12} + 2\bar{D}_{66})n^2 + \bar{B}_{12}]2\lambda^2 \\
 & + (2n^2\bar{D}_{26} + 2\bar{B}_{26} - \bar{D}_{26})2n\lambda + \bar{D}_{22}(n^2 - 1)^2 \\
 & + \bar{B}_{22}(2n^2 - 1) + 1
 \end{aligned} \tag{3.5i}$$

and

$$b_{11} = \lambda^2 K_2 + 2n\lambda K_3 + n^2 K_1 \tag{3.6a}$$

$$b_{12} = 0 \tag{3.6b}$$

$$b_{13} = \lambda K_1 \tag{3.6c}$$

$$b_{21} = b_{12} \tag{3.6d}$$

$$b_{22} = \lambda^2 K_2 + 2n\lambda K_3 + n^2 K_1 \tag{3.6e}$$

$$b_{23} = 2\lambda K_3 + nK_1 \quad (3.6f)$$

$$b_{31} = b_{13} \quad (3.6g)$$

$$b_{32} = b_{23} \quad (3.6h)$$

$$b_{33} = \lambda^2 K_2 + 2n\lambda K_3 + n^2 K_1 \quad (3.6i)$$

From equations (3.4), (3.5) and (3.6) it is evident that there are three equations corresponding to every integer  $n$  in the form:

$$\begin{bmatrix} a_{11} & a_{12} & a_{13} \\ a_{21} & a_{22} & a_{23} \\ a_{31} & a_{32} & a_{33} \end{bmatrix} \begin{bmatrix} U_n \\ V_n \\ W_n \end{bmatrix} - q \begin{bmatrix} b_{11} & b_{12} & b_{13} \\ b_{21} & b_{22} & b_{23} \\ b_{31} & b_{32} & b_{33} \end{bmatrix} \begin{bmatrix} U_n \\ V_n \\ W_n \end{bmatrix} = 0 \quad (3.7)$$

For numerical efficiency,  $U_n$  and  $V_n$  are eliminated from the above set of three equations, to get equation in  $W_n$ . Rewriting the first two equations as:

$$a_{11}U_n + a_{12}V_n + a_{13}W_n - q(b_{11}U_n + b_{12}V_n + b_{13}W_n) = 0 \quad (3.8a)$$

$$a_{12}U_n + a_{22}V_n + a_{23}W_n - q(b_{12}U_n + b_{22}V_n + b_{23}W_n) = 0 \quad (3.8b)$$

From equations (3.8), one has

$$\begin{aligned} U_n &= \frac{1}{(a_{11}a_{22} - a_{12}^2)} \{ (a_{12}a_{23} - a_{22}a_{13})_n W_n + \\ &\quad q [(a_{22}b_{11} - a_{12}b_{12})_n U_n + (a_{22}b_{12} - a_{12}b_{22})_n V_n \\ &\quad + (a_{22}b_{13} - a_{12}b_{23})_n W_n] \} \end{aligned} \quad (3.9a)$$

and

$$\begin{aligned}
 V_n = & \frac{1}{(a_{11}a_{22} - a_{12}^2)_n} \{ (a_{12}a_{13} - a_{23}a_{11})_n w_n + \\
 & q [(a_{11}b_{12} - a_{12}b_{11})_n u_n + (a_{11}b_{22} - a_{12}b_{12})_n v_n \\
 & + (a_{11}b_{23} - a_{12}b_{13})_n w_n] \} \quad (3.9b)
 \end{aligned}$$

Equations (3.9) can be used for an iteration which aims at obtaining  $U_n$  and  $V_n$  in terms of  $W_n$ . Iteration can be started by dropping the  $q$  terms, giving,

$$U_n = \frac{(a_{12}a_{23} - a_{13}a_{22})_n}{(a_{11}a_{22} - a_{12}^2)_n} w_n \quad (3.10a)$$

and,

$$V_n = \frac{(a_{12}a_{13} - a_{11}a_{23})_n}{(a_{11}a_{22} - a_{12}^2)_n} w_n \quad (3.10b)$$

Substituting equations (3.10) in (3.9) we obtain  $U_n$  and  $V_n$  in terms of  $W_n$  as:

$$\begin{aligned}
 U_n = & \frac{1}{(a_{11}a_{22} - a_{12}^2)_n} \{ (a_{12}a_{23} - a_{22}a_{13})_n w_n + \\
 & q [(a_{22}b_{11} - a_{12}b_{12})_n \frac{(a_{12}a_{23} - a_{13}a_{22})_n}{(a_{11}a_{22} - a_{12}^2)_n} w_n \\
 & + (a_{22}b_{12} - a_{12}b_{22})_n \frac{(a_{12}a_{13} - a_{11}a_{23})_n}{(a_{11}a_{22} - a_{12}^2)_n} w_n \\
 & + (a_{22}b_{13} - a_{12}b_{23})_n w_n] \} \quad (3.11a)
 \end{aligned}$$

and

With these definitions, equations (3.11) are rewritten as:

$$U_n = \left[ \frac{R_{1n}}{R_n} + q \left\{ \frac{R_{3n}R_{1n}}{R_n^2} + \frac{R_{4n}R_{2n}}{R_n^2} + \frac{R_{5n}}{R_n} \right\} \right] W_n \quad (3.12a)$$

and

$$V_n = \left[ \frac{R_{2n}}{R_n} + q \left\{ \frac{R_{6n}R_{1n}}{R_n^2} + \frac{R_{7n} + R_{2n}}{R_n^2} + \frac{R_{8n}}{R_n} \right\} \right] W_n \quad (3.12b)$$

Substituting equations (3.12) in the last equation of (3.7) and neglecting the higher order terms of  $q$ , the following form is obtained:

$$\begin{aligned} & a_{13n} \left[ \frac{R_{13}}{R_n} + q \left\{ \frac{R_{3n}R_{1n}}{R_n^2} + \frac{R_{4n}R_{2n}}{R_n^2} + \frac{R_{5n}}{R_n} \right\} \right] W_n \\ & + a_{23n} \left[ \frac{R_{2n}}{R_n} + q \left\{ \frac{R_{6n}R_{1n}}{R_n^2} + \frac{R_{7n}R_{2n}}{R_n^2} + \frac{R_{8n}}{R_n} \right\} \right] W_n \\ & + a_{33n} W_n - q [b_{31n} \frac{R_{1n}}{R_n} + b_{32n} \frac{R_{2n}}{R_n} W_n + b_{33n}] W_n = 0 \end{aligned} \quad (3.13)$$

This can be rewritten as

$$\begin{aligned} & \left[ \frac{a_{13}R_1 + a_{23}R_2}{R} + a_{33} \right] W_n - q [(b_{31}R_1 + b_{32}R_2 + b_{33} \right. \\ & \left. - R_5 - R_8)/R - (R_3R_1 + R_4R_2 + R_6R_1 + R_7R_2)/R^2] W_n = 0 \end{aligned} \quad (3.14)$$

Equation (3.14) represents a set of  $n$  linear homogeneous equations in  $W_n$  with  $q$  as the eigenvalue. These can be written as:

$$[A] \{W\} - q [B] \{W\} = 0 \quad (3.15)$$

$$\begin{aligned}
 V_n = & \frac{1}{(a_{11}a_{22} - a_{12}^2)_n} \{ (a_{12}a_{13} - a_{23}a_{11})_n w_n + \\
 & q [(a_{11}b_{12} - a_{12}b_{11})_n \frac{(a_{12}a_{23} - a_{13}a_{22})_n}{(a_{11}a_{22} - a_{12}^2)_n} w_n \\
 & + (a_{11}b_{22} - a_{12}b_{12})_n \frac{(a_{12}a_{13} - a_{11}a_{23})_n}{(a_{11}a_{22} - a_{12}^2)_n} w_n \\
 & + (a_{11}a_{23} - a_{12}a_{13})_n w_n] \} \quad (3.11b)
 \end{aligned}$$

Since further iteration of  $U_n$  and  $V_n$  yields an additional expression in terms of  $q^2$ , which is negligible as treated by Ugural and Cheng [15], equations (3.11) are taken as the final form.

For computational convenience, the following quantities are defined as:

$$R_{1n} = (a_{12}a_{23} - a_{22}a_{13})_n$$

$$R_{2n} = (a_{12}a_{13} - a_{11}a_{23})_n$$

$$R_{3n} = (a_{22}b_{11} - a_{12}b_{12})_n$$

$$R_{4n} = (a_{22}b_{12} - a_{12}b_{22})_n$$

$$R_{5n} = (a_{22}b_{13} - a_{12}b_{23})_n$$

$$R_{6n} = (a_{11}b_{12} - a_{12}b_{11})_n$$

$$R_{7n} = (a_{11}b_{22} - a_{12}b_{12})_n$$

$$R_{8n} = (a_{11}b_{23} - a_{12}b_{13})_n$$

and

$$R_n = (a_{11}a_{22} - a_{12}a_{12})_n$$

Subscript n in the above expressions implies the evaluation for specific value of n.

where,  $[A]$  and  $[B]$  are diagonal matrices with elements  $A_n$  and  $B_n$  given as:

$$A_n = \left[ \frac{a_{13}R_1 + a_{23}R_2}{R} + a_{33} \right]_n \quad (3.16a)$$

$$B_n = \left[ \frac{b_{31}R_1 + b_{32}R_2 + b_{33} - R_5 - R_8}{R} - \frac{R_3R_1 + R_4R_2 + R_6R_1 + R_7R_2}{R^2} \right]_n \quad (3.16b)$$

and  $\{W\}$  represents the column vector with elements  $w_1, w_2 \dots w_n$ .

### 3.4 Optimization

The objective of the present optimization study is to maximize the buckling strength of the laminated composite shell of specified geometry and weight. Such an optimization signifies the efficient use of composite laminates with different ply-angle orientations and ply thickness. The design variables here are fibre orientation and thickness of individual laminae. The number of layers of the shell is treated as a parameter, since, as a design variable it represents a mixed integer programming problem. Investigations are carried out for different loading combinations for the shell.

### 3.5 Problem Formulation

The optimization problem can be formulated as

$$\text{Maximize } (f(\alpha_i, h_i))$$

or

$$\text{Minimize } (-f(\alpha_i, h_i)) \quad i = 1, N$$

where,

$$f(\alpha_i, h_i) = \frac{q_{cr} L^2}{E_{LT} h^3}$$

$\alpha_i$  = orientation of  $i^{\text{th}}$  lamina

$h_i$  = thickness of  $i^{\text{th}}$  lamina

$N$  = No. of laminae

Subject to the following constraints:

- (i) lower bound and upper bound on the fibre orientation angle

$$0^\circ \leq \alpha_i \leq 90^\circ$$

- (ii) lower bound and upper bound on the lamina thickness  $h$

$$h_{i_{\min}} \leq h_i \leq h_{i_{\max}}$$

Here  $q_{cr}$  is the lowest eigenvalue obtained from the solution of equation (3.15).

### 3.6 Method of Optimization

Since the objective function for laminated composite cylindrical shells is quite a complicated function of design variables  $\alpha$  and  $h$ , constrained optimization method without using derivatives is suitable for solving the problem. The problem is to maximize the buckling load and find the fibre direction and lamina thickness at which buckling load is maximum.

For the constrained optimization solution without using derivatives, sequential augmented Lagrangian multiplier method is used. This method finds the minimum of a multivariable non-linear function subject to non-linear bounds, equality and inequality constraints. The formal statement of the method can be given as [23]

Minimize  $f(x_1, x_2, x_3, \dots, x_n)$

subject to

$$A_L < G_k(x_1, x_2, \dots, x_n) < A_u \quad k = 1, M$$

$$G_k(x_1, x_2, x_3, \dots, x_n) > 0.0 \quad k = M+1, M+N$$

$$G_k(x_1, x_2, x_3, \dots, x_n) = 0.0 \quad k = M+N+1, M+N+P$$

Optimization analysis was carried out using the programme E04UAF, supplied by Numerical Algorithm Group (NAG), available in the system library of DEC-1090 computer at IIT Kanpur.

The bounds on the constraints adopted in our case are as follows:

1. The angle of each ply is constrained between  $0^\circ$  and  $90^\circ$
2. The thickness of each laminae is constrained between 0.01 in. to 0.1 in., which being the practical range of commonly available laminae thicknesses.

### 3.7 Programming Procedure:

The main steps of programming procedure to determine the eigenvalue are as follows:

- \* For specified composite material properties and shell geometry the coefficients of stiffness matrices  $\bar{A}_{ij}$ ,  $\bar{B}_{ij}$  and  $\bar{D}_{ij}$  are computed.
- \* The coefficients  $a_{ij}$  and  $b_{ij}$  given by equations (3.5) and (3.6) are computed for each value of  $n$  ranging from 1 to 20.
- \* Parameters  $R, R_1 \dots R_8$  defined by equations (3.12) are computed and the diagonal matrices  $[A]$  and  $[B]$  given by equations (3.16) are obtained.

- \* Using NAG subroutine F02BJF available with DEC-1090 system the lowest eigenvalue solution of equation (3.15) is obtained.
- \* The procedure is repeated for values of  $m$  varying from 2 to 20, and the lowest value of buckling load is determined.

### 3.7a Steps of Optimization Procedure

- \* The initial design values of  $\alpha_i$  and  $h_i$  ( $i = 1, N$ ) are chosen within specified bounds and the value of  $q_{cr}$  using OBJECT subroutine is calculated.
- \* For obtaining the maximum value of  $q_{cr}$ , optimization is carried out using NAG subroutine E04UAF.
- \* The subroutine AMONIT is supplied for monitoring the optimization procedure, and is called at the end of every cycle of E04UAF.
- \* Values of  $\alpha_i$ 's and  $h_i$ 's at which the maximum value of  $q$  is obtained are given as the output along with the maximum value of  $q$ .

CHAPTER 4RESULTS AND DISCUSSION

In this chapter, the results on the buckling and optimization of shells are presented and discussed. Eigenvalue solution of equation (3.15) is obtained to get the buckling load for a shell of specified geometry subjected to all possible combinations of loadings. From this, a conclusion regarding the values of  $m$  and  $n$ , at which lowest eigenvalue occurs, is made. Next the effect of laminate configurations on buckling loads is studied. For shells of specified geometry six different configurations are studied and the results compared with those by Khot [11] who has used Donnell's theory. The effect of number of shell laminae on buckling loads is studied for a shell of specified geometry subjected to axial and pressure loadings and compared with Jones and Morgan [14] results who used Donnell's theory. Finally the effect of ply-angle orientations on buckling loads is done for shells of specified geometry. Results are compared with the ones obtained by Whitney and Sun [16], who also used Cheng-Ho theory with a different solution technique.

The computations have been carried out on DEC-1090 computer system at I.I.T. Kanpur. The material properties of composite materials which are used for numerical computations are given as follows:

Composite material	$E_L$ psi	$E_T$ psi	$G_{LT}$ psi	LT	TL
Boron Epoxy	$30.0 \times 10^6$	$3.0 \times 10^6$	$1.0 \times 10^6$	0.3	0.03
Graphite Epoxy	$30.0 \times 10^6$	$0.75 \times 10^6$	$3.75 \times 10^6$	0.25	0.00625
Carbon Epoxy	$20.0 \times 10^6$	$1.0 \times 10^6$	$0.6 \times 10^6$	0.25	0.0125

The definition of parameters  $K_1$ ,  $K_2$  and  $K_3$  used in the tables is reproduced for convenience:

$$q_1 = qK_1, \quad q_2 = qK_2 \quad \text{and} \quad q_3 = qK_3$$

All the buckling loads are obtained in terms of dimensionless parameter  $(qL^2/E_{LT})^{1/3} \times 10^2$ , where

$$q = N_x, \quad K_2 \neq 0 \quad \text{and} \quad K_1 = K_3 = 0$$

$$q = p, \quad K_1 \neq 0 \quad \text{and} \quad K_2 = K_3 = 0$$

$$q = T, \quad K_3 \neq 0 \quad \text{and} \quad K_1 = K_2 = 0$$

#### 4.1 Critical Buckling Load and Buckling Pattern:

Buckling loads are obtained for six layered Boron-Epoxy composite laminated shells under all possible loading combinations. The geometric properties used for this study are:

Length of shell : 60.0 in

Radius of shell : 5.0 in

Thickness of each lamina : 0.12 in

Table 4.1 gives the value of non-dimensional buckling load for the shell for specified values of  $m$  and  $n$  under

pressure loading. For each value of  $m$  and  $n$  was varied from 2 to 20 and  $m$  was varied from 1 to 20. The lowest buckling load of  $100.84 \times 10^2$  is obtained for  $m = 18$  and  $n = 12$ . In Figure 4.1 the variation of buckling load obtained as eigenvalue of equation (3.15) for specified values of  $m$  and  $n$ , with changing values of  $m$  and  $n$  is shown. Evidently, the range of variation of  $m$  and  $n$  chosen is sufficient to determine the buckling load.

Tables 4.2 and 4.3 give similar results to determine the critical values of the non-dimensional buckling load for the shell under axial load and torsion respectively. For the shell under axial compression the value of critical buckling load is  $18.95 \times 10^2$ , occurring at  $m = 18$  and  $n = 12$ . In the case of torsional loading, the value of critical buckling load is  $9.38 \times 10^2$ , occurring at  $m = 18$  and  $n = 12$ . In Figures 4.1 and 4.2 the buckling loads are plotted for different value of  $m$  and  $n$ .

Table 4.4 gives critical values of non-dimensional buckling load for shell subjected to combined loading ( $K_1 = 1$ ,  $K_2 = 1$ ,  $K_3 = 1$ ). The non-dimensional critical buckling load is found to be  $2.91 \times 10^2$  at  $m = 18$  and  $n = 10$ . In Figure 4.4 the buckling loads are plotted for each value of  $m$  and  $n$ .

Similar computations are carried out for all possible cases of loadings and these result are concisely given in Table 4.5. From these results it is seen that for case of single loadings the buckling pattern is  $m = 18$  and  $n = 12$ , and for case of combined loadings the buckling pattern is

$m = 18$  and  $n = 10$ . This observation is very significant. It was later used in optimization problem which requires repeated determination of the eigenvalue. Using the values of  $m$  and  $n$  obtained here, direct comparisons are made with the results obtained by Khot [11], discussed later.

From Table 4.5 it is observed that torsional load affects the buckling of the shell most strongly. The effects of axial load and pressure load are in descending order.

#### 4.2 Effect of Laminate Configurations on Buckling Load:

The shell considered for this study has the following properties:

Composite material	:	Boron Epoxy
Number of layers	:	3
Length of shell	:	72.0 in
Radius of shell	:	6.0 in
Thickness of laminae	:	0.012 in.

Types of configurations studied are:

- a)  $-\alpha, 0, \alpha$       b)  $-\alpha, \pi/2, \alpha$       c)  $0, \alpha, -\alpha$
- d)  $\pi/2, \alpha, -\alpha$       e)  $\alpha, -\alpha, 0$       f)  $\alpha, -\alpha, \pi/2$ .

Type of loading considered in all the cases is combined axial load, pressure and torsion.

Tables 4.6, 4.7 and 4.8 show the effect of the various configurations on the values of buckling loads. The results were obtained using  $m = 18$  and  $n = 10$ . These results are compared with the results by Khot [11] who used Donnell's theory of shells.

The results by Khot are 20% higher than the experimental ones. The fact that present results are more close to experimental results by about 10-12% implies that Cheng-Ho theory gives result which are significantly better than those obtained by Donnell's theory. Figures 4.5 and 4.6 show the variation of buckling loads with ply orientations for different configurations. The configurations  $-\alpha$ ,  $0$ ,  $\alpha$  and  $-\alpha$ ,  $\pi/2$ ,  $\alpha$  give maximum buckling load as obtained by Khot at  $\alpha = 60^\circ$  and  $\alpha = 30^\circ$  respectively. This gives us an added confidence in the validity of Cheng-Ho theory and the improvements it shows over Donnell's theory.

#### 4.3 Effect of Number of Shell Laminae on Buckling Loads:

The shell considered for this study has the following material and geometric properties:

Composite material	:	Boron Epoxy
Length of shell	:	34.64 in
Radius of shell	:	10.0 in
Thickness of laminae	:	0.12 in
Orientation of laminae	:	$[0/90]_s$

Table 4.9 gives the variation of buckling loads with the number of shell laminae. Two cases of single loadings - axial compression and pressure - are considered. Figure 4.7 shows the variation of non-dimensional buckling load with the number of laminae. It is observed that for pressure loading, the buckling load constantly increases with increase in number of layers; while for axial loading at  $N = 10$ , the buckling load

is maximum after which it decreases. For directly comparing the present results with the ones obtained by Jones and Morgan [14] the non-dimensional parameter for axial load is reduced to the form used by them. It is seen that the results by the present theory are less by about 15% as compared to the ones by Jones and Morgan who used Donnell's theory.

#### 4.4 Effect of Ply-angle Orientations on Buckling Loads:

The shell considered for this study has the following material and geometric properties:

Composite material	:	Carbon Epoxy
Number of laminae	:	4
Length of shell	:	60.0 in
Radius of shell	:	6.0 in
Thickness of laminae	:	0.12 in

Table 4.10 gives the values of non-dimensional buckling loads for shells subjected to axial and torsional load singly. For the various configurations of ply-angle orientations, a reasonable agreement is found with the values of buckling loads obtained by Whitney and Sun [16] who used Cheng and Ho equations and obtained the buckling load by employing double Fourier series expansion for the displacement functions. The material and geometric properties considered here are identical to the ones used by Whitney and Sun. The difference in the results by Whitney and Sun and present theory show that the deviation of one results is significant on the lower side thus approaching the experimental conditions. Also the solution technique used

in the present work is a single series expansion in which the size of matrices for computation of eigenvalues is considerably reduced. This reduces computation time considerably.

From the results of Sections 4.1, 4.2, 4.3 and 4.4 the improvement of Cheng-Ho theory over Donnell's theory is established for the ease of long shells. Comparison with the results obtained by Whitney and Sun validates the method used to obtain the solution using Cheng-Ho theory. Reasonable agreement with the available results [16] justifies the use of  $m = 18$  and  $n = 12$  for single loadings and  $m = 18$ ,  $n = 10$  for combined loadings.

#### Optimization Results:

Results are compared with the one's obtained by Hirano [19] who has used Donnell's theory. Study is done for all cases of combined loadings, and for varying length-to-radius ratios of the shell. The effects of fixed lamina thickness and variable lamina thickness on maximum buckling load are also studied.

Optimization study is done to maximize the buckling strength of laminated composite shells of specified geometry and weight. The design variables there are fibre orientations and ply thickness of individual laminae. Number of layers of the shell is treated as a parameter.

#### 4.5 Optimum Buckling Loads for Fixed and Variable Lamina Thickness:

The shell considered for this study has the following material and geometric properties:

$$L = 60.0 \text{ in}, \quad L/a = 10.0, \quad t = 0.8 \text{ in}, \quad N = 6.$$

Table 4.11 gives the values of optimum buckling load for different length-to-radius ratios of the shell subjected to all cases of combined loadings. Each lamina is considered to be of equal thickness and the values of ply-orientation angles are obtained at the maximum buckling load. By varying length-to-radius ratios of the shell it is observed that as this ratio increases the maximum buckling load decreases. This is due to increase in effective bending stiffness of shell. The values of buckling loads for the combined loading conditions yields the values of  $\alpha$  which are less than those for loads acting singly. The general trend is similar to that observed in Section 4.1.

Table 4.12 gives the values of optimum buckling loads for the shells with thickness of each lamina variable. At the optimal point the laminate configuration turns out to be very close to antisymmetric laminate.

It is observed that the ratio  $t_2/t_3 \approx 3.05$  and  $t_1/t_3 \approx 1.49$  for each case of loading is independent of the length-to-radius ratio of the shell. For six layered laminates, the optimal thicknesses ratios, satisfy the relation

$$R_2 = (R_1 - 1) + 2(R_1^2 + 1)^{1/2}$$

$$\text{where } R_2 = t_2/t_3 \text{ and } R_1 = t_1/t_3$$

for antisymmetric angle ply laminates. This was obtained by Sharma [23] to predict decoupling in antisymmetric laminates.

#### 4.6 Effect of Starting Point on Optimal Buckling Loads:

The shell considered for this study has the following material and geometric properties:

Composite material : Boron-Epoxy

$N = 6$ ,  $L = 60.0$  in,  $L/a = 10.0$ ,  $t = 0.8$  in

The effect of starting point on the optimum solution of a six-layered laminated shell for  $L/a$  ratio of 10.0 is shown in Table 4.13. The case of axial loading is considered. It is seen that with different starting points the fibre orientations of plies come out different, but the change in non-dimensional buckling load is very small. In the case of starting point  $\alpha_i$ 's = 45°, the value of the load differs significantly. For comparing the results obtained by Hirano [19] who has used Donnell's theory, the non-dimensional buckling load parameter is reduced to the form used by Hirano [19]. The results obtained by Hirano are 60-65% more than the experimental results. The present results show a significant improvement on Hirano's results i.e. results are closer to experimental result by 15.7%. Moreover Hirano has assumed the thickness of plies to be pre-assigned and equal, and found maximum buckling load, treating fibre orientation as the only variable. In the present work, as given in Table 4.14 thicknesses are also treated as design variables to search for an improved design. It is seen that at the optimal solution, laminate tends to become antisymmetric with thickness ratios to decouple the laminate. Hardly any effect of starting points on the optimal load is observed. Thickness variation increases the load carrying capacity by 10-12%.

Table 4.1

98878

Values of critical buckling loads and buckling patterns for six-layered Boron-Epoxy composite laminated shell under pressure loading

m	n	$qL^2/E_{LT}t^3 \times 10^2$	m	n	$qL^2/E_{LT}t^3 \times 10^2$
10	6	111.83	16	6	107.00
	8	110.96		8	105.38
	10	109.22		10	104.71
	12	107.68		12	103.42
	14	106.75		14	102.52
	16	105.40		16	101.41
	18	104.86		18	101.21
	20	104.42		20	101.08
<hr/>					
12	6	110.43	18	6	106.31
	8	108.01		8	104.60
	10	107.14		10	102.79
	12	105.53		12	100.84
	14	104.82		14	101.47
	16	104.21		16	101.41
	18	103.99		18	102.87
	20	103.98		20	104.82
<hr/>					
14	6	108.57	20	6	105.81
	8	106.54		8	103.27
	10	106.13		10	102.09
	12	104.97		12	101.86
	14	103.93		14	101.01
	16	102.51		16	102.38
	18	102.12		18	103.71
	20	101.98		20	103.66

Table 4.2

Values of critical buckling loads and buckling pattern for six-layered Boron-Epoxy composite laminated shells under axial compression

m	n	$qL^2/E_{LT}t^3 \times 10^2$	m	n	$qL^2/E_{LT}t^3 \times 10^2$
10	6	20.68	16	6	19.94
	8	20.49		8	19.81
	10	20.22		10	19.61
	12	20.05		12	19.54
	14	19.84		14	19.42
	16	19.60		16	19.25
	18	19.55		18	19.16
	20	19.40		20	19.00
-----					
12	6	20.50	18	6	19.47
	8	20.42		8	19.30
	10	20.37		10	19.15
	12	19.94		12	18.95
	14	19.69		14	19.04
	16	19.55		16	19.33
	18	19.37		18	19.36
	20	19.23		20	19.37
-----					
14	6	20.21	20	6	19.40
	8	19.97		8	19.37
	10	19.79		10	19.30
	12	19.65		12	19.11
	14	19.31		14	19.08
	16	19.20		16	18.99
	18	19.11		18	18.99
	20	19.08		20	19.04

Table 4.3

Values of critical buckling loads and buckling patterns for six-layered Boron-Epoxy composite laminated shells under torsion

m	n	$qL^2/E_{LT}t^3 \times 10^2$	m	n	$qL^2/E_{LT}t^3 \times 10^2$
10	6	15.51	16	6	11.21
	8	14.67		8	11.02
	10	14.20		10	10.94
	12	14.00		12	10.74
	14	13.86		14	10.68
	16	13.79		16	10.21
	18	13.52		18	10.08
	20	13.21		20	10.13
-----					
12	6	14.30	18	6	10.38
	8	13.38		8	9.61
	10	12.79		10	9.38
	12	12.66		12	9.38
	14	12.42		14	9.40
	16	12.12		16	9.51
	18	12.30		18	9.78
	20	12.47		20	9.92
-----					
14	6	12.40	20	6	10.08
	8	11.39		8	9.43
	10	11.00		10	9.39
	12	10.80		12	9.50
	14	10.78		14	9.60
	16	10.61		16	9.81
	18	10.60		18	9.86
	20	10.81		20	9.96

Table 4.4

Values of critical buckling loads and buckling pattern for six-layered Boron-Epoxy composite laminated shells under combined axial, pressure and torsional loadings

m	n	$qL^2/E_{LT}t^3 \times 10^2$	m	n	$qL^2/E_{LT}t^3 \times 10^2$
10	6	5.54	16	6	3.72
	8	5.22		8	3.51
	10	5.18		10	3.19
	12	4.88		12	3.01
	14	4.41		14	2.96
	16	4.18		16	2.96
	18	4.00		18	2.99
	20	3.83		20	3.31
<hr/>					
12	6	5.30	18	6	3.41
	8	5.11		8	3.32
	10	5.03		10	2.91
	12	4.51		12	2.92
	14	4.33		14	2.96
	16	4.20		16	3.34
	18	4.01		18	3.84
	20	3.74		20	3.86
<hr/>					
14	6	4.91	20	6	3.21
	8	4.61		8	3.08
	10	4.38		10	3.00
	12	4.00		12	2.97
	14	3.68		14	2.94
	16	3.26		16	2.92
	18	3.01		18	2.96
	20	3.14		20	2.98

Table 4.5

Critical buckling loads and buckling patterns for a six-layered Boron-Epoxy composite laminated shell subjected to different type of loadings

$K_1$	$K_2$	$K_3$	$m$	$n$	$qL^2/E_{LT}t^3 \times 10^2$
1	0	0	18	12	100.844
0	1	0	18	12	18.955
0	0	1	18	12	9.382
1	1	0	18	10	18.767
1	0	1	18	10	19.103
0	1	1	18	10	6.778
1	1	1	18	10	2.914

Table 4.6

Values of critical buckling load for three-layered Boron-Epoxy shell ( $K_1 = 1$ ,  $K_2 = 1$ ,  $K_3 = 1$ )

Configuration	$\alpha$	Critical buckling load ( $q_{cr}$ lb/in)		Percentage difference
		Results by Khot [11]	Results by present study	
$-\alpha, 0, \alpha$	10	937	859.97	8.27
	20	1062	954.55	10.16
	30	1000	905.70	9.43
	40	1000	905.30	9.47
	50	1100	978.78	11.02
	60	1375	1214.67	11.66
	70	1250	1095.25	12.38
	80	1000	896.73	10.33
	90	900	727.64	8.04
	-----	-----	-----	-----
$\alpha, \pi/2, \alpha$	0	850	747.06	12.11
	10	1000	876.41	12.36
	20	1200	1057.08	11.91
	30	1300	1138.02	12.46
	40	1150	994.29	13.54
	50	1050	913.39	13.01
	60	1050	916.33	12.73
	70	1150	1033.16	10.16
	80	1050	947.62	9.75
	90	1000	928.80	7.12

Table 4.7

Values of critical buckling load for three-layered Boron-Epoxy shell ( $K_1 = 1$ ,  $K_2 = 1$ ,  $K_3 = 1$ )

Configuration	$\alpha$	Critical buckling load ( $\alpha_{cr}$ 1b/in)		Percentage difference
		Results by Khot [11]	Results by present study	
0, $\alpha$ , $-\alpha$	10	512	464.08	9.36
	20	567	498.99	11.21
	30	512	463.72	9.43
	40	487	448.72	7.86
	50	487	450.62	7.47
	60	512	461.67	9.83
	70	567	503.66	11.17
	80	512	463.51	9.47
	90	500	470.25	5.95
-----				
$\pi/2$ , $\alpha$ , $-\alpha$	0	500	439.21	12.16
	10	515	442.85	14.01
	20	575	507.20	11.79
	30	515	462.93	10.11
	40	475	430.92	9.28
	50	475	430.68	9.33
	60	515	470.65	8.61
	70	575	514.79	10.47
	80	515	469.83	8.77
	90	500	454.72	9.06

Table 4.8

Values of critical buckling load for three-layered Boron-Epoxy shell ( $K_1 = 1$ ,  $K_2 = 1$ ,  $K_3 = 1$ )

Configuration	$\alpha$	Critical buckling load ( $q_{cr}$ lb/in)		Percentage difference
		Results by Khot [11]	Results by present study	
$\alpha, -\alpha, 0$	10	475	426.74	10.16
	20	500	457.93	8.42
	30	510	451.29	11.51
	40	525	463.78	11.86
	50	537	474.83	11.66
	60	510	460.43	9.72
	70	500	460.40	7.92
	80	495	455.15	8.05
	90	475	427.16	10.07
$\alpha, -\alpha, \pi/2$	0	480	445.10	7.28
	10	485	437.85	9.73
	20	500	442.95	11.41
	30	515	457.94	11.08
	40	535	469.62	12.22
	50	540	473.96	12.23
	60	535	478.39	10.58
	70	515	459.79	10.72
	80	505	460.76	8.76
	90	500	453.95	9.21

Table 4.9

Variation of critical buckling load with number of shell laminae for cross-ply laminated Boron-Epoxy shells

Number of layers	$pL^2/E_{LT}t^3 \times 10^2$		Percentage difference	$pL^2/E_{LT}t^3 \times 10^2$
	Results by Jones and Morgan [14]	Present results		
3	17.33	14.73	14.98	94.16
5	18.65	15.85	15.1	98.73
7	20.15	17.25	14.37	107.22
9	20.38	17.87	12.29	116.70
10	20.83	17.85	14.31	118.39
20	20.18	17.82	11.73	131.44
25	20.08	17.66	12.05	138.21
30	19.51	16.56	15.11	146.08
50	18.72	15.87	15.23	172.86

Table 4.10

Variation of buckling load with ply-angle orientations for four-layered carbon epoxy laminated shells

Laminate configuration	Non-dimensional buckling load ( $qL^2/E_{LT}t^3$ ) $\times 10^2$						
	Axial load			Torsional load			
	Results by Whitney & Sun [16]	Present results	Percentage difference	Results by Whitney & Sun [16]	Present results	Percentage difference	
[0/0] <sub>s</sub>	11.6	12.0	+3.5	1.8	1.6	-12.5	
[15/0] <sub>s</sub>	15.0	15.2	+1.3	1.9	2.0	+5.0	
[30/0] <sub>s</sub>	18.4	17.4	-5.75	2.8	3.2	+12.9	
[45/0] <sub>s</sub>	22.2	20.8	-6.73	6.0	5.0	-20.0	
[60/0] <sub>s</sub>	23.6	21.2	-11.3	7.1	6.4	+11.3	
[75/0] <sub>s</sub>	21.0	20.5	-2.4	9.1	8.0	-13.75	
[90/0] <sub>s</sub>	18.0	18.2	+1.1	8.4	7.8	-7.69	

Optimum values of buckling loads for six-layered Boron Epoxy laminated shells with equal laminae thickness, subject to different loading conditions

K <sub>1</sub> Pressure	K <sub>2</sub> (Axial comp.)	K <sub>3</sub> (Torsion)	L/a Ratio	Ply orientations				Non-dimensional buckling load: (qL <sup>2</sup> /ELt <sup>3</sup> ) x 10 <sup>2</sup>
				θ <sub>1</sub>	θ <sub>2</sub>	θ <sub>3</sub>	θ <sub>4</sub>	
0	0	8.0	11.36	-32.41	17.22	-21.31	43.37	-9.61
		10.0	31.19	-48.17	52.18	60.06	40.43	19.78
		12.0	19.47	-37.04	18.27	34.26	41.14	16.21
1	0	8.0	26.75	-18.73	68.01	-50.16	21.44	32.21
		10.0	-28.21	43.11	69.72	-73.18	50.11	34.67
		12.0	31.29	-39.56	33.05	-42.55	31.18	-26.48
0	1	8.0	9.16	-34.21	45.03	-36.18	41.32	-12.31
		10.0	17.42	-58.02	89.41	-64.52	73.16	-15.42
		12.0	11.34	-34.78	70.21	-60.19	42.36	17.10
1	1	8.0	27.42	-33.18	19.07	-11.21	39.50	-18.31
		10.0	43.21	-45.08	49.16	-47.11	46.23	-48.06
		12.0	51.23	-18.43	67.18	-72.36	22.45	41.71
1	0	8.0	9.43	11.17	15.42	-18.76	21.15	-13.34
		10.0	19.72	-39.76	51.03	57.11	43.18	16.65
		12.0	48.36	63.14	32.00	79.79	59.24	-41.06
0	1	8.0	17.36	-31.14	47.21	-50.17	36.39	-19.55
		10.0	-34.18	-60.78	74.11	-72.01	-62.71	38.71
		12.0	40.01	38.14	42.06	45.11	39.04	-41.85
1	1	8.0	19.74	-28.36	42.18	-47.07	30.72	-20.33
		10.0	24.71	-47.02	39.11	-40.76	39.22	-28.73
		12.0	33.13	-46.63	54.23	-61.39	51.40	-38.26

Table 4.12

values of buckling loads for six-layered Boron-Epoxy, angle-ply laminated shell subjected to different loading conditions

$K_3$	$L/a$	Fibre orientations						Lamina thickness				$\frac{qL^2}{E_{LT}t^3} \times 10^2$		
		$\theta_1$	$\theta_2$	$\theta_3$	$\theta_4$	$\theta_5$	$\theta_6$	$t_1$	$t_2$	$t_3$	$t_4$	$t_5$	$t_6$	$\frac{qL^2}{E_{LT}t^3} \times 10^2$
0	8.0	32.6	-30.1	32.6	-33.1	28.7	-33.4	0.1081	0.2213	0.0726	0.0721	0.2201	0.1081	30.035
0	10.0	43.6	-45.4	43.6	-42.1	47.6	-40.3	0.1081	0.2206	0.0731	0.0711	0.2208	0.1079	24.459
0	12.0	44.8	-46.6	44.8	-44.3	47.0	-45.3	0.1083	0.2214	0.0726	0.0718	0.0221	0.1081	22.736
-	-	-	-	-	-	-	-	-	-	-	-	-	-	
0	8.0	36.22	-28.4	36.27	-35.12	31.00	-36.3	0.1081	0.2203	0.0722	0.0731	0.2211	0.1084	14.3.003
0	10.0	51.83	-47.77	51.83	-52.06	45.00	-52.15	0.1084	0.2211	0.0730	0.0716	0.2205	0.1078	120.421
0	12.0	57.16	-52.30	59.5	-58.9	53.16	-53.2	0.1086	0.2225	0.0710	0.0710	0.2211	0.1085	116.370
-	-	-	-	-	-	-	-	-	-	-	-	-	-	
0	8.0	31.48	-28.21	36.24	-35.12	24.18	-36.43	0.1084	0.2261	0.0723	0.0711	0.2200	0.1083	25.979
1	10.0	62.44	-58.33	63.17	-66.5	60.23	-64.15	0.1082	0.2243	0.0715	0.0718	0.2215	0.1077	20.431
1	12.0	61.37	-60.48	61.38	-60.4	63.16	-60.13	0.1081	0.2210	0.0726	0.0715	0.2206	0.1074	19.072
-	-	-	-	-	-	-	-	-	-	-	-	-	-	
0	8.0	18.37	-27.43	19.06	-20.48	30.11	-18.17	0.1081	0.2211	0.0728	0.0721	0.2214	0.1088	28.432
0	10.0	54.71	-50.32	58.99	-60.18	49.76	-53.22	0.1078	0.2207	0.0721	0.0711	0.2219	0.1080	21.114
0	12.0	69.48	-76.21	68.23	-67.14	76.13	-70.05	0.1076	0.2214	0.0727	0.0716	0.2208	0.1076	19.213
-	-	-	-	-	-	-	-	-	-	-	-	-	-	
1	10.0	56.18	-49.18	56.27	-49.18	50.21	-58.21	0.1083	0.2208	0.0711	0.0711	0.2216	0.1081	18.353
1	12.0	73.42	-61.03	72.16	-71.14	61.03	-70.43	0.1081	0.2216	0.0720	0.0711	0.2204	0.1081	16.991
-	-	-	-	-	-	-	-	-	-	-	-	-	-	
1	8.0	21.72	-16.34	22.04	-21.00	17.86	-24.11	0.1081	0.2214	0.0710	0.0716	0.2218	0.1083	17.328
1	10.0	66.14	-78.79	67.32	-69.13	80.21	-64.35	0.1036	0.2211	0.0713	0.0723	0.2200	0.1086	14.541
1	12.0	83.11	-78.26	82.14	-80.16	79.32	-84.51	0.1089	0.2203	0.0721	0.0724	0.2216	0.1078	12.048
-	-	-	-	-	-	-	-	-	-	-	-	-	-	
1	8.0	28.42	-11.76	27.14	-25.0	12.13	-30.0	0.1081	0.2214	0.0714	0.0714	0.2213	0.1071	11.126
1	10.0	39.28	-58.01	37.41	-37.55	54.13	-39.19	0.1033	0.2221	0.0721	0.0716	0.2222	0.1075	8.353
1	12.0	63.42	-38.35	62.07	-60.44	39.18	-65.18	0.1079	0.2217	0.0726	0.0720	0.2214	0.1078	7.461

Table 4.13

Effect of starting point on optimal buckling loads and ply-angle orientations for six-layered boron-Epoxy laminated shell with equal laminae thickness, subjected to axial loading

$$\text{Buckling load parameter } \beta = \frac{N_x \cdot \sqrt{3} R}{t^2}$$

Set No.	Ply-angle orientation					$\beta_{\text{Hi rano}} [19]$	$\beta_{\text{present work}}$	Percentage difference
	$\theta_1$	$\theta_2$	$\theta_3$	$\theta_4$	$\theta_5$			
1	S	0.0	0.0	0.0	0.0	0.0	21.873	1.2054x10 <sup>7</sup>
	F	16.31	0.83	-1.7	-2.41	0.97	18.42	1.0320x10 <sup>7</sup>
2	S	10.0	30.0	30.0	30.0	30.0	21.683	1.0117x10 <sup>7</sup>
	F	18.62	-17.41	22.10	-32.40	19.86	27.35	8.8351x10 <sup>6</sup>
3	S	45.0	45.0	45.0	45.0	45.0	21.416	5.1014x10 <sup>7</sup>
	F	43.17	40.28	47.16	49.04	41.28	43.74	5.5801x10 <sup>6</sup>
4	S	60.0	60.0	60.0	60.0	60.0	21.971	-
	F	-42.17	31.73	17.43	-21.51	33.72	50.16	1.0369x10 <sup>7</sup>
5	S	90.0	90.0	90.0	90.0	90.0	21.880	1.2054x10 <sup>7</sup>
	F	54.21	63.11	72.43	61.21	80.43	52.19	1.0331x10 <sup>7</sup>
6	S	90.0	0.0	90.0	0.0	90.0	92.076	1.2369x10 <sup>7</sup>
	F	31.19	-48.17	52.18	60.06	40.43	19.78	1.0711x10 <sup>7</sup>
7	S	90.0	0.0	45.0	45.0	0.0	22.076	1.2369x10 <sup>7</sup>
	F	31.19	-48.17	52.18	60.06	40.43	19.78	1.0711x10 <sup>7</sup>
8	S	0.0	0.0	45.0	45.0	0.0	22.013	1.2479x10 <sup>7</sup>
	F	24.14	16.18	-12.21	52.17	18.14	29.17	1.0552x10 <sup>7</sup>
9	S	30.0	45.0	90.0	90.0	45.0	30.0	21.961
	F	27.16	42.30	78.14	-72.16	51.04	28.11	-
10	S	15.0	45.0	60.0	60.0	45.0	15.0	21.565
	F	9.08	-31.63	43.17	51.48	-31.00	7.04	2.150 x 10 <sup>5</sup>

63

I<sub>axial</sub> = 1

Effect of starting point on optimal buckling loads, fibre orientations and laminae thickness for  
six-layered Boron-Epoxy laminated shells under axial loading

o.	Ply-angle orientation						Lamine thickness				Non-dimensional buckling load ( $qL^2/E_{LT} t^3$ ) $\times 10^2$		
	$\theta_1$	$\theta_2$	$\theta_3$	$\theta_4$	$\theta_5$	$\theta_6$	$t_1$	$t_2$	$t_3$	$t_4$	$t_5$	$t_6$	
S	0.0	0.0	0.0	0.0	0.0	0.0	0.0	0.0	0.0	0.0	0.0	0.0	24.455
F	16.73	-0.97	1.83	-1.79	0.84	-15.31	0.1079	0.2211	0.0728	0.0731	0.2203	0.1079	24.455
S	30.0	30.0	30.0	30.0	30.0	30.0	30.0	30.0	30.0	30.0	30.0	30.0	24.430
F	20.42	-18.31	24.50	-23.99	18.92	-20.63	0.1081	0.2208	0.0720	0.0128	0.2213	0.1031	24.430
S	45.0	45.0	45.0	45.0	45.0	45.0	45.0	45.0	45.0	45.0	45.0	45.0	24.421
F	43.08	-40.71	45.01	-45.06	40.66	-43.24	0.1081	0.2197	0.0731	0.0724	0.2201	0.1032	24.421
S	60.0	60.0	60.0	60.0	60.0	60.0	60.0	60.0	60.0	60.0	60.0	60.0	24.449
F	48.27	-39.73	50.16	-48.37	39.04	-47.18	0.1077	0.2194	0.0708	0.0711	0.2193	0.1086	24.449
S	90.0	90.0	90.0	90.0	90.0	90.0	90.0	90.0	90.0	90.0	90.0	90.0	24.457
F	53.16	-60.43	70.43	-71.67	61.25	-52.71	0.1079	0.2206	0.0714	0.0717	0.2204	0.1078	24.457
S	90.0	0.0	90.0	0.0	90.0	0.0	90.0	0.0	90.0	0.0	90.0	0.0	24.451
F	38.17	-18.36	60.21	-58.93	15.31	-38.17	0.1081	0.2214	0.0726	0.0723	0.2209	0.1080	24.451
S	90.0	0.0	45.0	45.0	0.0	90.0	0.0	90.0	0.0	90.0	0.0	90.0	24.474
F	42.14	-17.06	51.88	-52.91	18.21	-43.00	0.1083	0.2210	0.0729	0.0731	0.2210	0.1081	24.474
S	0.0	0.0	45.0	45.0	0.0	0.0	0.0	0.0	0.0	0.0	0.0	0.0	24.456
F	8.73	-12.48	39.60	-37.11	13.74	-9.7	0.1081	0.2216	0.0714	0.0725	0.2220	0.1085	24.456
S	30.0	45.0	90.0	90.0	45.0	30.0	30.0	30.0	30.0	30.0	30.0	30.0	24.459
F	43.6	-45.4	43.6	42.11	45.3	41.3	0.1081	0.2206	0.0731	0.0711	0.2208	0.1079	24.459
S	15.0	45.0	60.0	60.0	45.0	15.0	15.0	15.0	15.0	15.0	15.0	15.0	24.406
F	10.81	-31.18	57.40	-56.46	33.33	-10.03	0.1076	0.2210	0.0716	0.0709	0.2213	0.1080	24.406

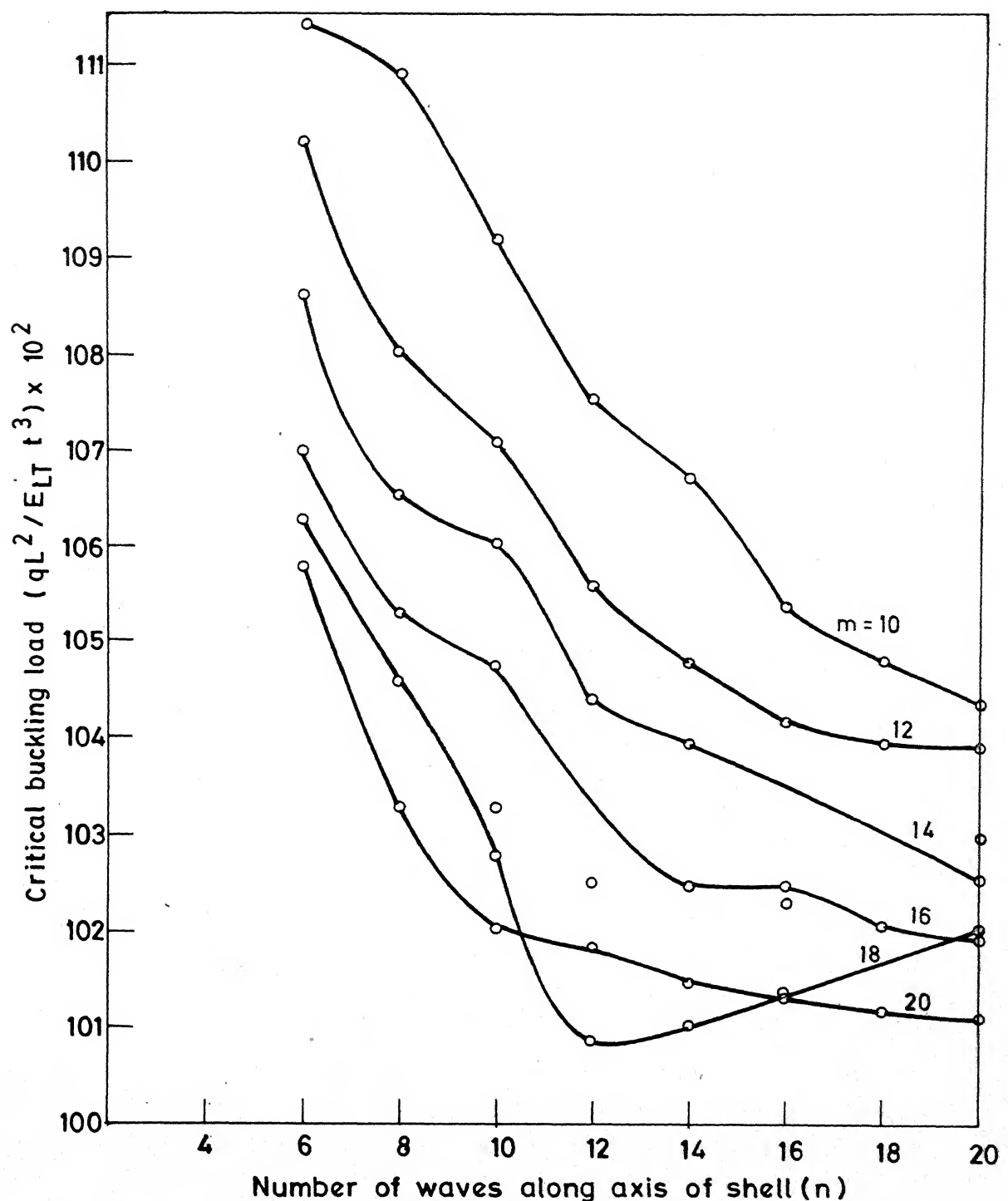


FIG. 4.1 CRITICAL BUCKLING LOAD AND BUCKLING PATTERN FOR SIX-LAYERED BORON-EPOXY COMPOSITE SHELL UNDER PRESSURE LOADING

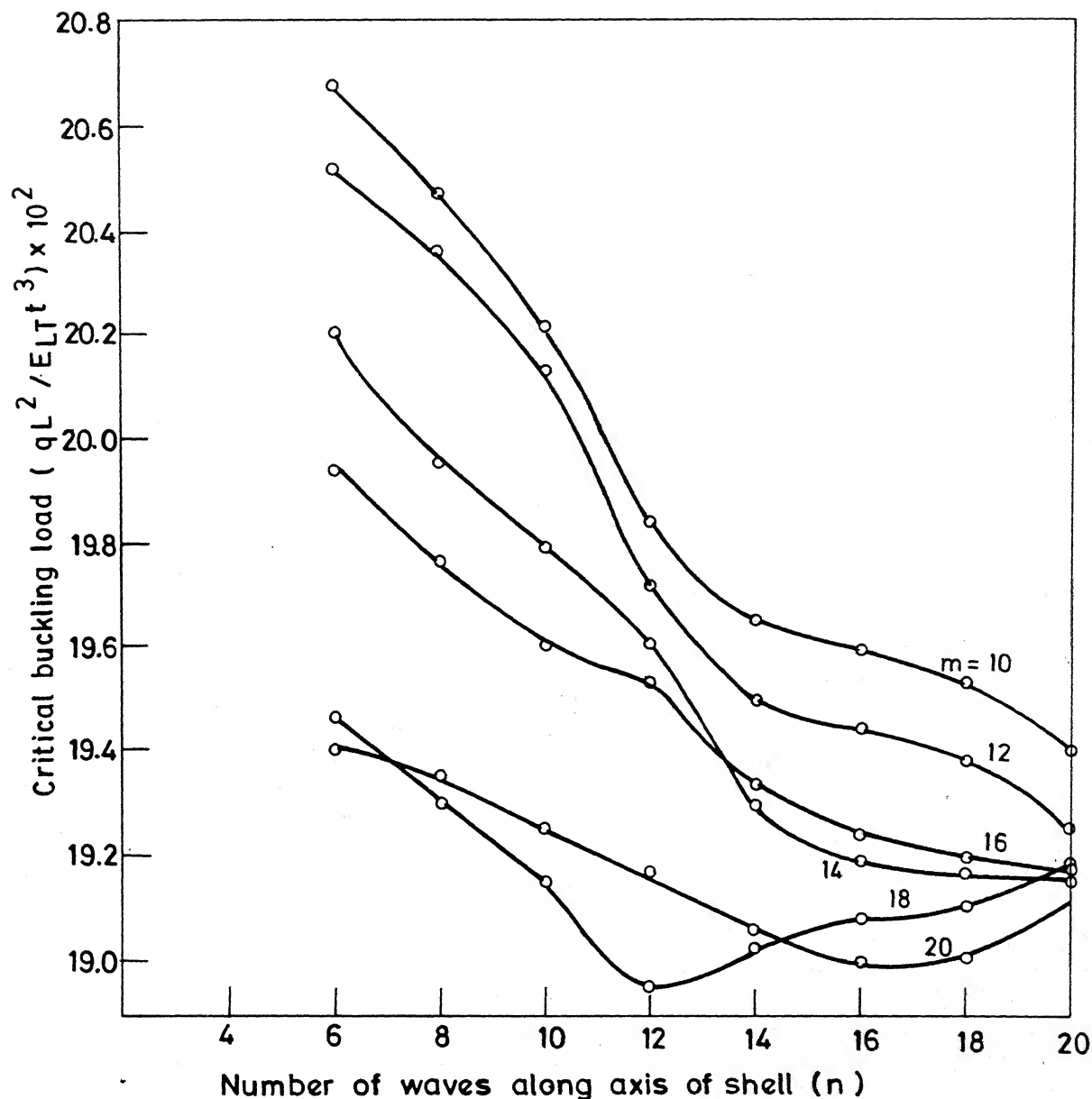


FIG. 4.2 CRITICAL BUCKLING LOAD AND BUCKLING PATTERN FOR SIX-LAYERED BORON-EPOXY COMPOSITE SHELL UNDER AXIAL COMPRESSION

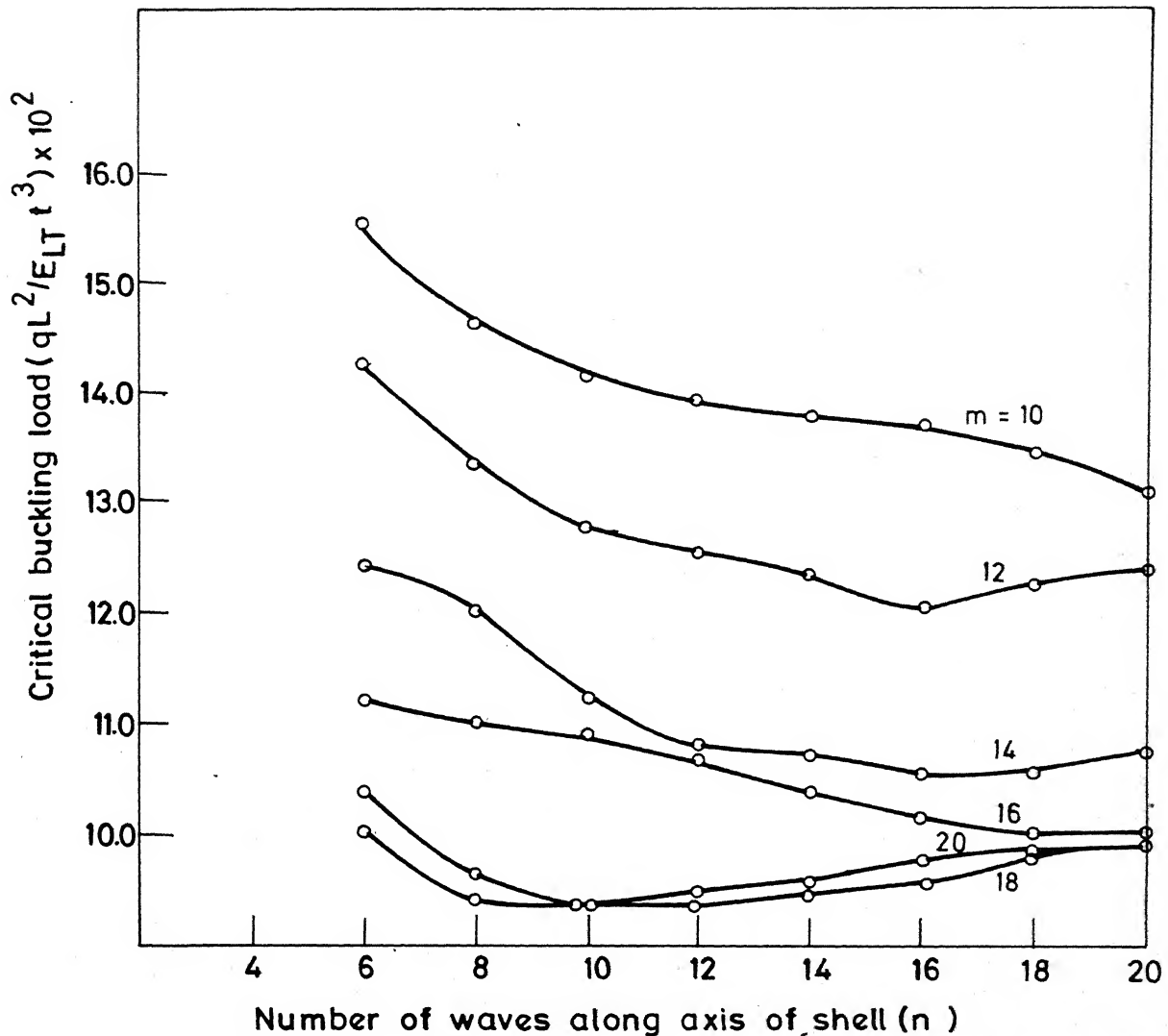


FIG. 4.3 CRITICAL BUCKLING LOAD AND BUCKLING PATTERN FOR SIX-LAYERED BORON-EPOXY COMPOSITE SHELL UNDER TORSION

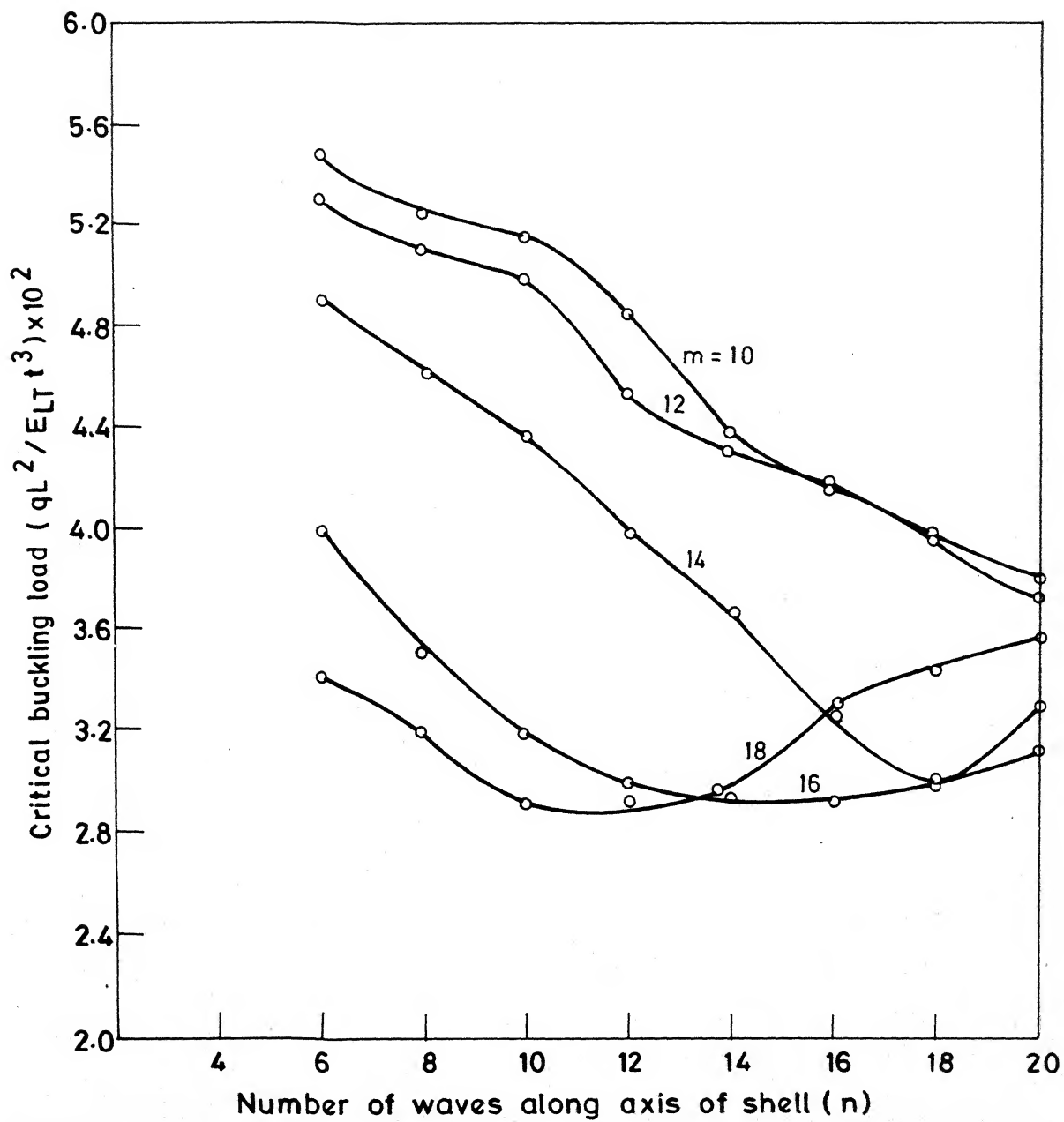


FIG. 4.4 CRITICAL BUCKLING LOAD AND BUCKLING PATTERN FOR SIX-LAYERED BORON-EPOXY COMPOSITE SHELL UNDER COMBINED AXIAL COMPRESSION, PRESSURE AND TORSION

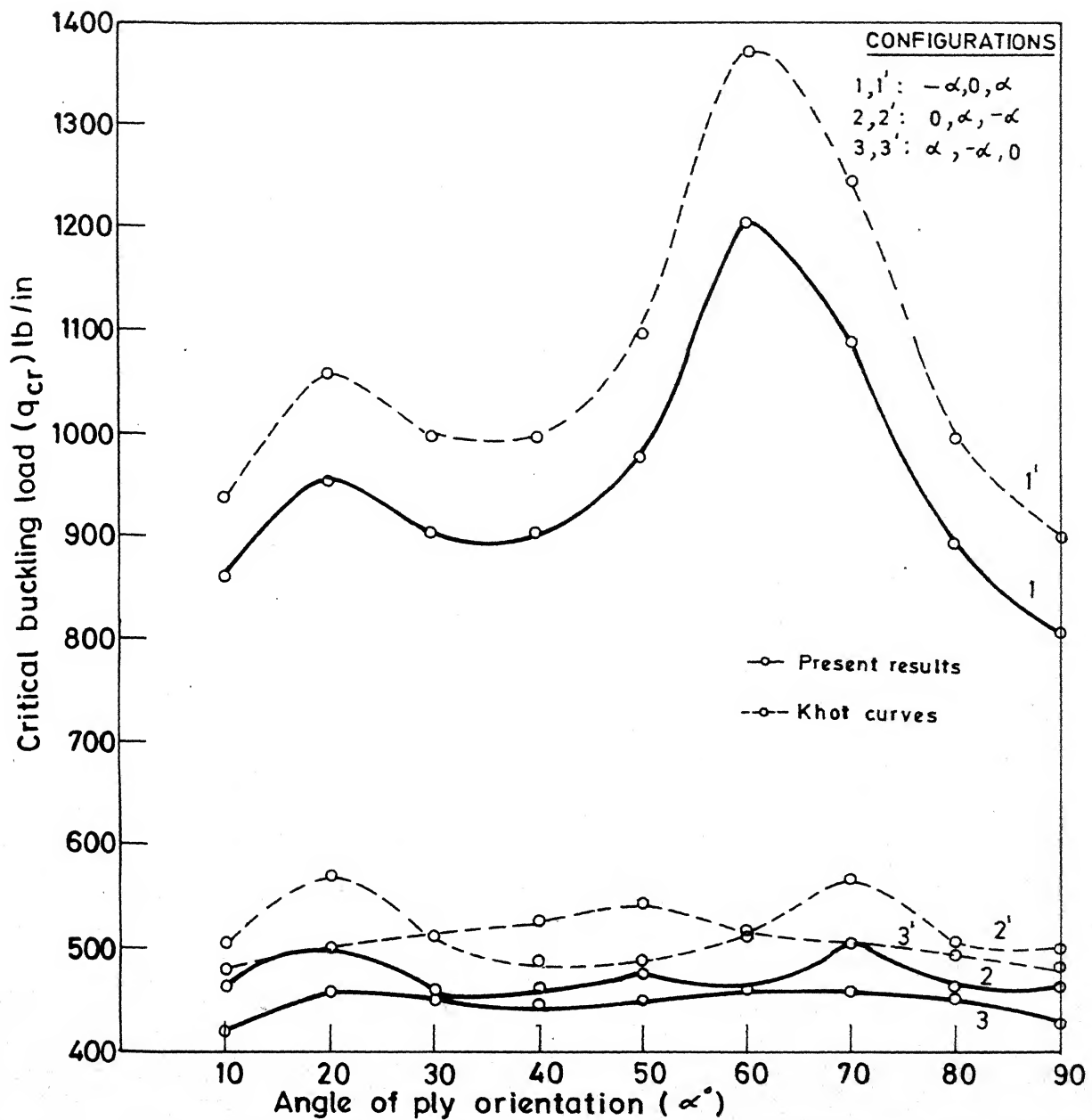


FIG. 4.5 EFFECT OF VARIOUS LAMINATE CONFIGURATIONS ON CRITICAL BUCKLING LOAD FOR 3-LAYERED BORON-EPOXY SHELL

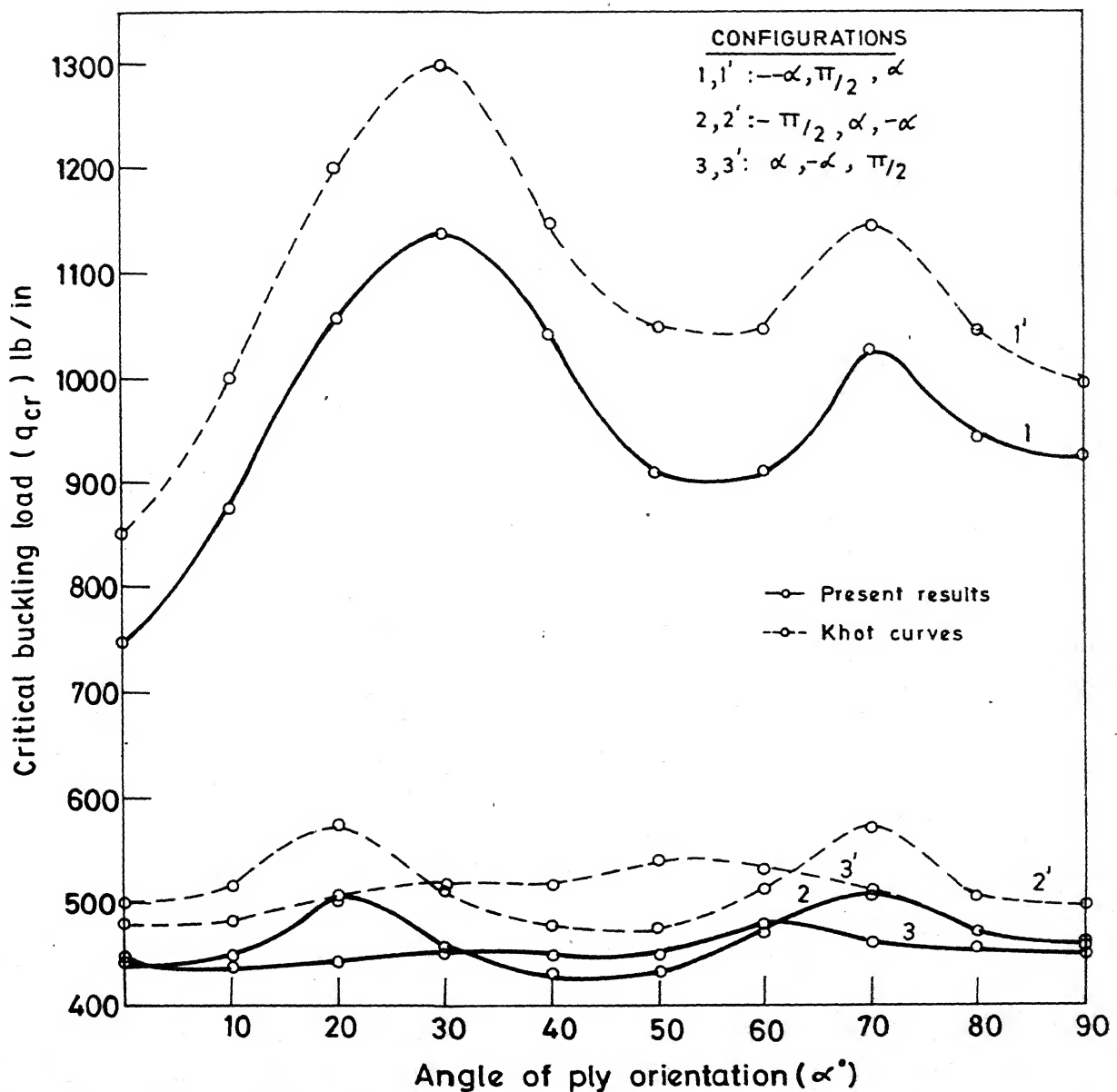


FIG. 4.6 EFFECT OF VARIOUS LAMINATE CONFIGURATIONS ON CRITICAL BUCKLING LOAD FOR 3-LAYERED BORON-EPOXY SHELL

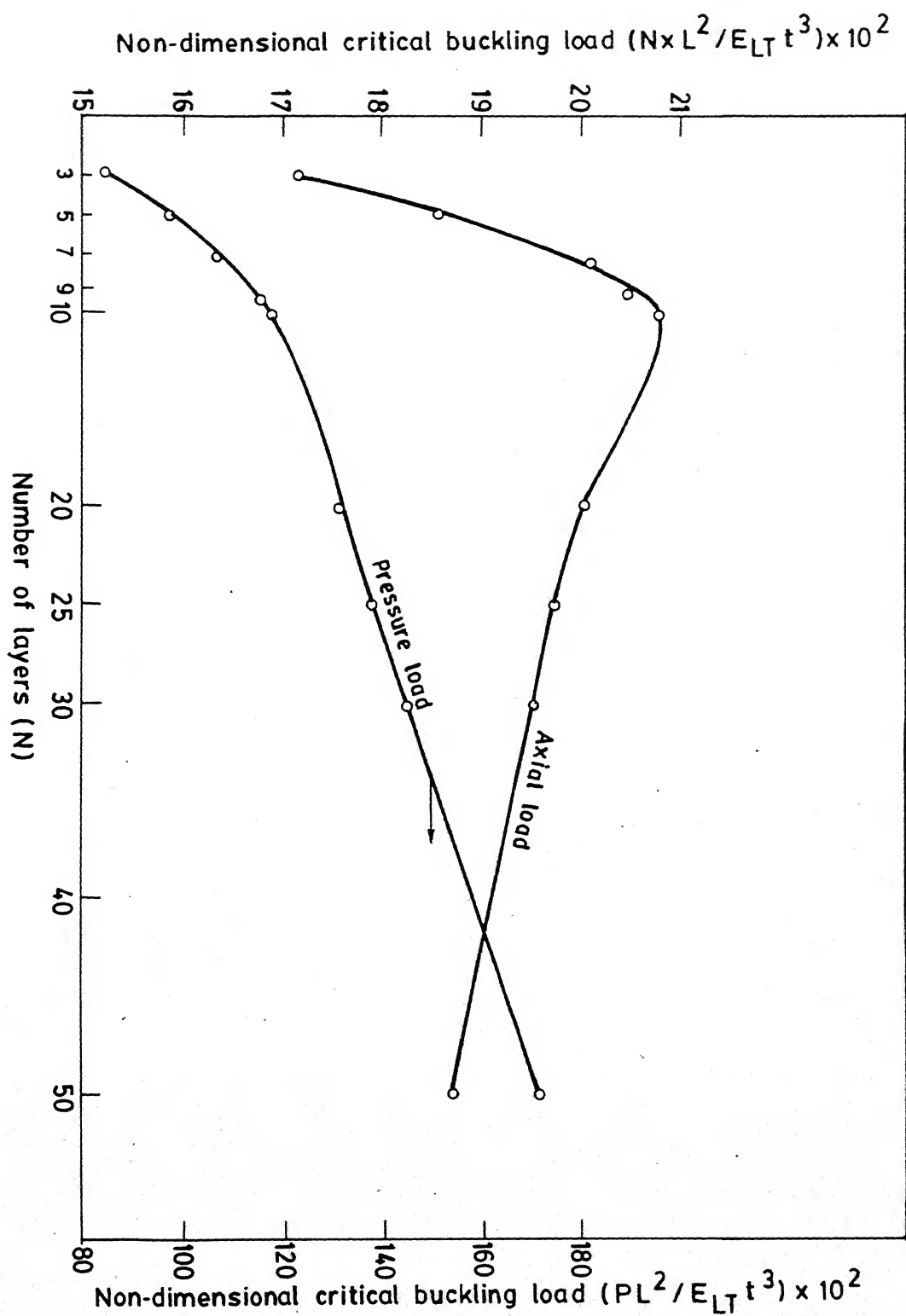


FIG. 4.7  
EFFECT OF NUMBER OF SHELL LAMINAЕ ON CRITICAL BUCKLING LOAD  
FOR CROSS-PLY LAMINATED BORON-EPOXY SHELL

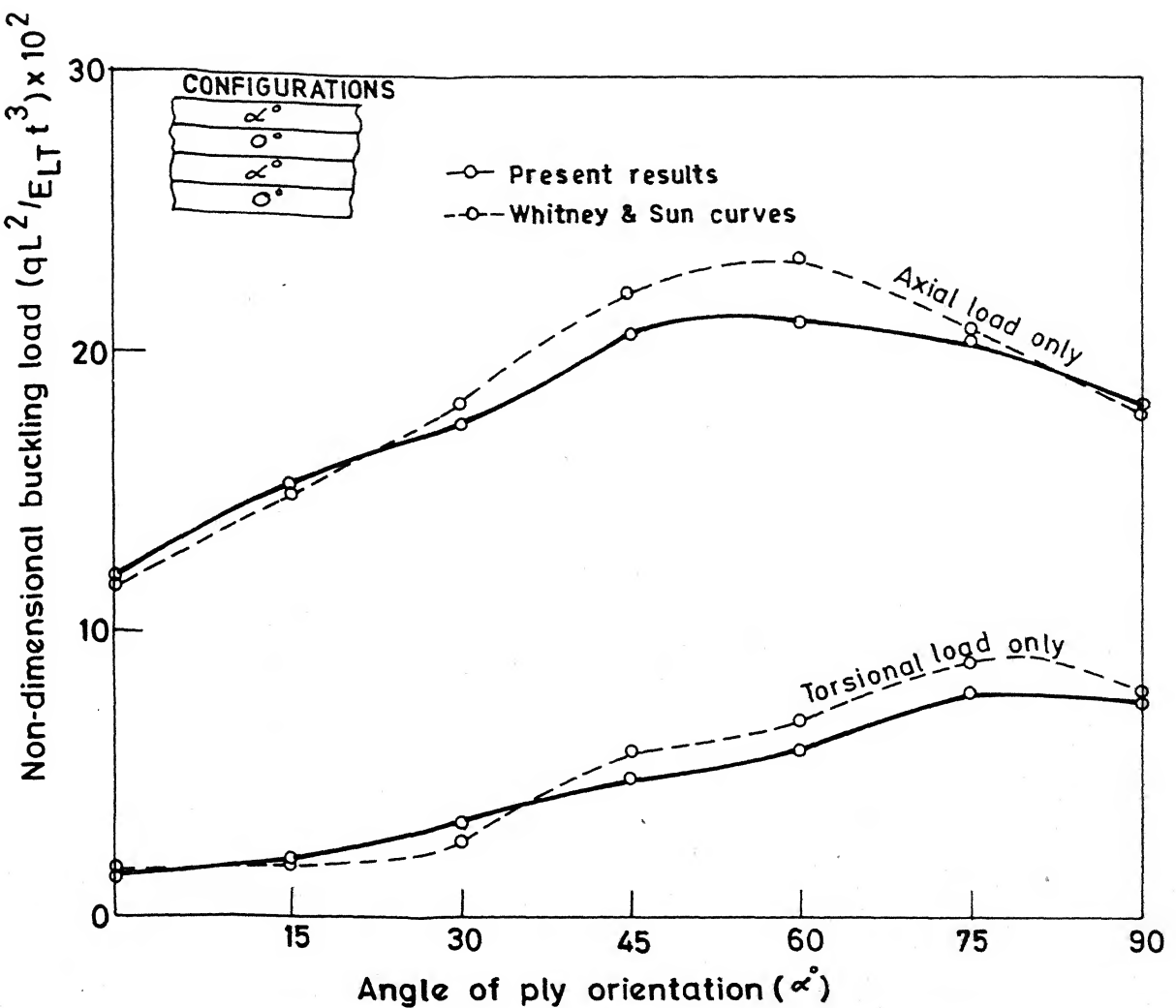


FIG. 4.8 EFFECT OF PLY-ANGLE ORIENTATIONS ON CRITICAL BUCKLING LOAD FOR 4-LAYERED CARBON EPOXY LAMINATED SHELL

## CHAPTER 5

### CONCLUSIONS

On the basis of the results obtained on the present work, the following general conclusions can be drawn:

- \* The buckling of six layered composite laminated shells subjected to single loadings is found to occur at values of  $m = 18$  and  $n = 12$ . In case of combined loadings, buckling is found to occur at values of  $m = 18$  and  $n = 10$ . The solution technique adopted does not allow the satisfaction of any boundary conditions. Thus Cheng and Ho theory with this form of solution technique can be used for the analysis of laminated composite shells, with good reliability.
- \* By studying the effect of various laminate configurations on buckling load and comparing the results by those obtained by Khot [11] who has used Donnell's theory, it is concluded that the use of Cheng and Ho theory gives results closer to experimental values by about 10-15%, as compared to the results obtained using Donnell's theory.
- \* The study of effect of number of cross-ply shell laminae on buckling loads indicates that for the case of axial loading, with the increase of number of laminae upto 10, the buckling load increases, after which it falls. In case

of pressure loading the buckling load increases with increase in number of laminae.

- \* The study of effect of ply-angle orientations on buckling loads indicate a reasonably good comparison of the present results with those by Whitney and Sun [16] who have used Cheng-Ho theory with the solution in form of double Fourier series expansion. The major advantage of using the solution technique adopted in the present work is that computer time for numerical calculations is greatly reduced, and the results obtained are closer to the experimental values.
- \* As length-to-radius ratio of the shell increases, the maximum buckling load of the antisymmetric six-layered shells decreases.
- \* For six-layered antisymmetric angle-ply laminated shells subjected to all combinations of loadings, the thickness ratios  $t_2/t_3 \approx 3.05$  and  $t_1/t_3 \approx 1.5$  have constant values independent of length-to-radius ratio and loading conditions. At the optimal point laminate is antisymmetric with thickness ratios producing a decoupled laminate. Thus an antisymmetric, uncoupled six-layered laminated shell has the maximum buckling load carrying capacity.
- \* Effect of starting point on optimal solution indicates the existence of different sets of ply orientations leading to almost the same buckling load.
- \* In case of laminated composite shells, best fibre directions cannot be obtained, but it is seen that at the optimum point, the values of maximum buckling load are constant.

- \* Optimization of buckling load with ply-thickness and orientations as design parameters increases buckling load by about 12% over the case when laminae thickness is uniform.

LIST OF REFERENCES

1. Budiansky, B., "Notes on non-linear shell theory", *Journal of Applied Mechanics*; Vol. 35; 1968; pp. 393-402.
2. Mah, G.B., Almroth, B.O., Pittner, E.V., "Buckling of orthotropic cylinders", *AIAA Journal*; Vol. 6; 1968; pp. 598-602.
3. Tennyson, R.C., "Buckling of circular cylindrical shells in axial compression", *AIAA Journal*; Vol. 2; 1964; pp. 1351-1353.
4. Becker, H., Gerard, G., "Elastic stability of orthotropic shells", *Journal of Aerospace Sciences*; Vol. 29, 1962; pp. 505-512.
5. Dong, S.B., Pister, K.S., Taylor, R.L., "On the theory of laminated anisotropic shells and plates", *Journal of Aerospace Sciences*; Vol. 29; 1962; pp. 969-975.
6. Tsai, J., "Effect of heterogeneity on the stability of composite cylindrical shells under axial compression", *AIAA Journal*; Vol. 4; 1966; pp. 1058-1062.
7. Serapico, J.C., "Elastic stability of orthotropic cylindrical shells subjected to axisymmetric loading", *AIAA Journal*; Vol. 1; 1963; pp. 128-138.
8. Lowe, G.G., "Structural analysis of orthotropic shells", *AIAA Journal*; Vol. 4; 1966; pp. 1843-1849.
9. Dow, N.F., Rosen, B.W., "Structural efficiency of orthotropic cylindrical shells subjected to axial compression", *AIAA Journal*; Vol. 4; 1963; pp. 481-490.
10. Weingarten, V.I., "Effects of internal pressure on the buckling of circular cylindrical shells under bending", *Journal of Aerospace Sciences*; Vol. 29; 1962; pp. 804-813.
11. Khot, N.S., "Buckling behavior of composite cylindrical shells under axial compression", *AIAA Journal*; Vol. 8; 1970; pp. 229-239.
12. Cheng, S., Ho, B.P.C., "Stability of heterogeneous aleotropic cylindrical shells under combined loading", *AIAA Journal*; Vol. 1; 1963; pp. 892-898.
13. Cheng, S., Ho, B.P.C., "Some problems in stability of heterogeneous aleotropic cylindrical shells under combined loading", *AIAA Journal*; Vol. 1; 1963; pp. 1603-1606.

14. Jones, R.M., Morgan, H.S., "Buckling of cross-ply laminated circular cylindrical shells", AIAA Journal; Vol. 13; 1975; pp. 664-673.
15. Ugural, A.C., Cheng, S., "Buckling of composite cylindrical shells under pure bending", AIAA Journal; Vol. 6; 1968; pp. 349-354.
16. Whitney, J.M., Sun, C.T., "A refined theory for laminated anisotropic cylindrical shells", Journal of Composite Materials; Vol. 41; 1975; pp. 471-482.
17. Nshanian, Y.S., Pappas, M., "Optimal laminated composite shells for buckling and vibrations", AIAA Journal; Vol. 21; 1983; pp. 403-438.
18. Hirano, Y., "Buckling of angle-ply laminated circular cylindrical shells", Journal of Applied Mechanics; Vol. 46; 1980; pp. 233-234.
19. Hirano, Y., "Optimization of laminated composite plates and shells", Composite Materials - Recent Advances; Pergamon Press, N.Y.
20. Flügge, W., "Stresses in shells", Springer-Verlag, Berlin; pp. 433-483.
21. Calcote, L.R., "The analysis of laminated composite structures", Van Nostrand Reinhold Company, New York; pp. 143-151.
22. Jones, R.M., "Buckling of circular cylindrical shells with different modulii in tension and compression", AIAA Journal; Vol. 9; 1971; pp. 53-57.
23. Sharma, S. et.al., "A study of coupling in laminated plates", Fibre Science & Technology, An International Journal; Vol. 18; No. 4; 1983.

AE-1907-M-TAM-CPT

98878